# Synthesis and electrochemical properties of slipped-cofacial porphyrin dimers of ferrocene-functionalized Zn-imidazolyl-porphyrins as potential terminal electron donors in photosynthetic models†

**Dipak Kalita, Mitsuhiko Morisue and Yoshiaki Kobuke***

*Received (in Durham, UK) 17th May 2005, Accepted 13th October 2005*
*First published as an Advance Article on the web 10th November 2005*
**DOI: 10.1039/b506992k**



A systematic series of ferrocene-functionalized Zn-imidazolyl-porphyrins were synthesized to assemble into the slipped-cofacial porphyrin dimers through imidazolyl-to-zinc complementary coordination as artificial photosynthetic models. Direct substitution at the *meso* position of the porphyrin ring with ferrocence and octamethylferrocene leads to the characteristic electronic structures, while the ferrocene substituents through phenylene-ethenylene and phenylene-ethylene spacers mitigate the electronic communications. Bathochromic shift of Q band, fluorescence quenching, and redox potentials of porphyrin ring are rationalized by the degree of electron-donating ability of the terminal ferrocenes.

## Introduction

The slipped-cofacial arrangement of natural pigments plays an important role in achieving efficient energy and electron transfer reactions with excellent yields in photosynthetic systems. In the natural systems, light energy conversion is carried out by several chromophores that are fixed and arranged closely to each other in the membrane protein.[1] The photosynthesis process is initiated by the absorption of sunlight by the light-harvesting antenna complexes where rapid and efficient energy transfer takes place over many pigments until eventually reaching the reaction center. In the reaction center,[2] there is a "special pair" of bacteriochlorophyll dimer where the photoinduced charge separation helps convert the harvested solar energy. As shown by the X-ray crystal structures of the bacterial photosynthetic reaction center, the most prominent characteristics of the "special pair" are the slipped-cofacial arrangements of the two bacteriochlorophylls and their electronic coupling.[2,3] The beautiful structural arrangement of natural photosynthetic systems have motivated many chemists throughout the world to design artificial photosynthetic models to study its complex energy/electron transfer mechanism and its underlying basic principles.[4]

The introduction of an imidazolyl group at the *meso* position of a porphyrin led to the spontaneous formation of a "slipped-cofacial porphyrin dimer" by the complementary coordination of the imidazolyls to the central Zn(II) in each porphyrin (Scheme 1).[5] The structural model developed by our research group mimics the geometry of natural photosystems by including complementary imidazolyl-to-zinc coordination, and enables two chromophoric $\pi$-orbitals to interact strongly in a slipped-cofacial arrangement. It served not only as a special pair model, but also as a building block of circular and linear porphyrin arrays, providing materials for both light-harvesting antenna complexes[6] and non-linear optics[7] models. However, the slipped-cofacial dimer structure can undergo exchange reactions and dissociate in the presence of competing ligands such as 1-methylimidazole, pyridine and MeOH. These properties enable the structures to be reorganized after their formation and allow the creation of a range of supramolecular systems by self-assembly. These supramolecular approaches have many advantages from the point of view of organic synthesis. Based on a deeper understanding of photoinduced electron-transfer reactions provided by model systems, laboratories hope to design systems for converting solar energy into chemical potential with simpler supramolecular techniques that use ITO (indium-tin oxide) electrode surface. In view of this, Zn-imidazolyl-porphyrin dyads were functionalized with five different types of ferrocenes to give **2-ZnD**–**6-ZnD** as shown in Scheme 1. Methylation increased the electron donating character of the ferrocene core in comparison with that of the unsubstituted ferrocene group and led to potential terminal electron donor groups for model photosynthetic devices. Systematically changing the group linking the ferrocene and the porphyrin may allow the elucidation of the effect of electronic communication between the two chromophores, not only in the present imidazolyl-porphyrins but in porphyrins generally. All electrochemical and spectral analyses of ferrocene-functionalized Zn-imidazolyl-porphyrins (**2-ZnD**–**6-ZnD**) were compared to the reference samples **1-ZnD** and **1-Zn-Im**, which lack ferrocenyl groups (Scheme 1).

Ferrocene was chosen as the electron donor group in the present study because the electron transfer from ferrocene is known to be very fast[8] and its redox active properties and those of its derivatives have been thoroughly investigated by several groups.[9] Ferrocene generates a relatively stable cation.

*Graduate School of Materials Science, Nara Institute of Science and Technology, 8916-5 Takayama, Ikoma 630-0192, Japan. E-mail: kobuke@ms.naist.jp; Fax: (+81)743-72-6119; Tel: (+81)743-72-6110*

† Electronic supplementary information (ESI) available: preparation of **11**, $^1$H and $^{13}$C NMR spectra, MALDI-TOF mass spectra, UV-Visible absorption and steady state emission spectra of all ferrocenyl porphyrin derivatives. See DOI: 10.1039/b506992k

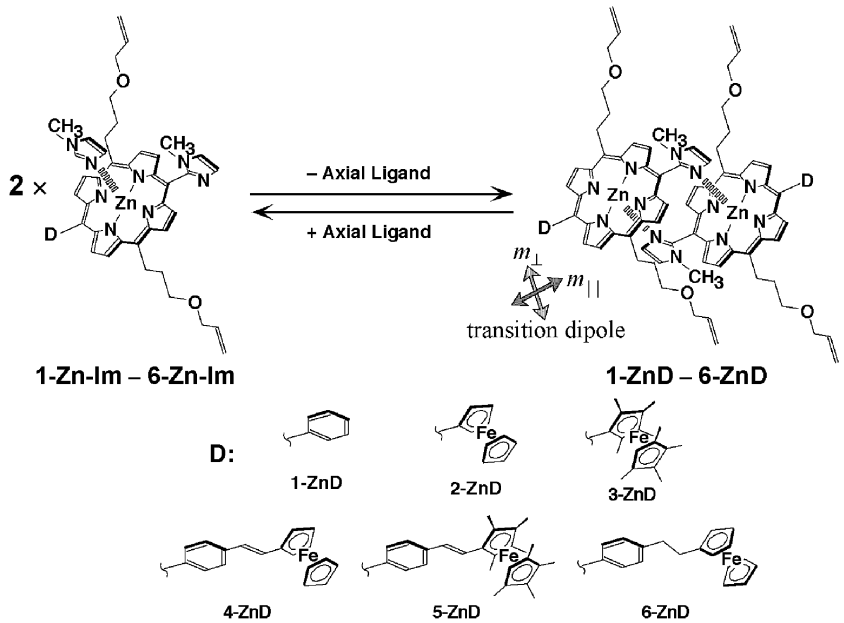


**Scheme 1** Schematic representation of the dimer–monomer equilibrium of ferrocene-functionalized Zn imidazolyl-porphyrins.



The electrochemical potential of which can be tuned by introducing appropriate substituents, thus affording oxidation potentials in the range of −0.2 V to > +0.5 V.[10] However, in comparison to the well-developed chemistry of ferrocene and its numerous applications[11] in organic synthesis, homogeneous catalysis and materials science, the analogous chemistry of methylated ferrocene derivatives is limited.[12]

Each of the target porphyrins bears three different *meso* substituents ($AB_2C$ type) including imidazolyl. Two of the porphyrins, **2-ZnD** and **3-ZnD**, are connected directly to ferrocene or 2,2′,3,3′,4,4′,5,5′-octamethylferrocene by covalent bonds, respectively. The other two porphyrins, **4-ZnD** and **5-ZnD**, have an intervening phenylene-ethenylene spacer between the porphyrin and the ferrocenyl or 2,2′,3,3′,4,4′,5,5′-octamethyl ferrocenyl substituent, respectively. In compounds **4-ZnD** and **5-ZnD**, the phenylene bridges are connected directly to the porphyrin ring so that they may serve as spacer groups allowing rotation of the ferrocenyl and octamethylferrocenyl groups while providing a fixed distance between the donor and the acceptor groups. Using Cerius 2 software (Ver. 4.6/Force Field UNIVERSAL 1.02), the center-to-center (Zn–Fc) distance was calculated to be 13.67 Å. In **6-ZnD**, direct conjugation between the porphyrin and the ferrocene group was cut off. In each of the five porphyrins, one of the *meso*-positions is substituted by a 1-methylimidazole group which allows assembly of the molecule into a slipped-cofacial dimer through complementary coordination to the central Zn(II). The remaining two *meso*-positions (5, 15 positions) are substituted with allyloxy ether groups, this enables the complementary dimer pair to be covalently linked by a ring closing olefin metathesis reaction.[6c,17] The ferrocene-functionalized Zn-imidazolyl-porphyrin dyads thus synthesized, **2-ZnD** to **6-ZnD**, can be tuned by the addition of competing ligands, as shown in Scheme 1.

Although the literature provides the syntheses of several ferrocene substituted porphyrins,[13] to our knowledge this is the first time that a sterically hindered octamethylferrocene group has been introduced at the *meso*-position of a porphyrin by means of a covalent bond or *via* a spacer unit. Likewise, there have been no previous reports of porphyrins having both imidazolyl and ferrocenyl subunits.

It is intended to use these substituted porphyrins to construct hetero-redox systems on transparent ITO electrodes by the complementary coordination of thiol-substituted Zn-imidazolyl-porphyrins with ferrocene-functionalized Zn-imidazolyl-porphyrins, followed by the formation of a covalent linkages by ring closing metathesis using Grubbs catalyst. This is an extension of our research towards photocurrent generation,[14,15] the details of which will be published elsewhere.[16] In the present study, we focus on the synthesis of the ferrocenyl-appended Zn-imidazolyl-porphyrins, **2-ZnD** to **6-ZnD**, and the effect of dimerization on their electrochemical properties. The monomeric reference compounds of these ferrocenyl-appended Zn-imidazolyl-porphyrins, **2-Zn-Im** to **6-Zn-Im**, were also prepared using 1-methylimidazole, as shown in Scheme 1. The electrochemical behavior of the ferrocenyl-appended Zn-imidazolyl-porphyrins and the monomeric reference compounds were compared to each other.

## Results and discussions

### Synthesis

The synthesis of the reference sample **1-ZnD** was described in our previous report.[17] The synthetic routes for the ferrocene-functionalized Zn-imidazolyl-porphyrins, **2-ZnD** to **6-ZnD**, are shown in Scheme 2.

**Ferrocene directly-linked porphyrins, 2-ZnD and 3-ZnD.** Directly linked porphyrin-ferrocene dyads **2-ZnD** and **3-ZnD** were synthesized by the mixed condensation of the ferrocene carboxaldehyde with the corresponding *meso*-(3-allyloxypropyl)

 

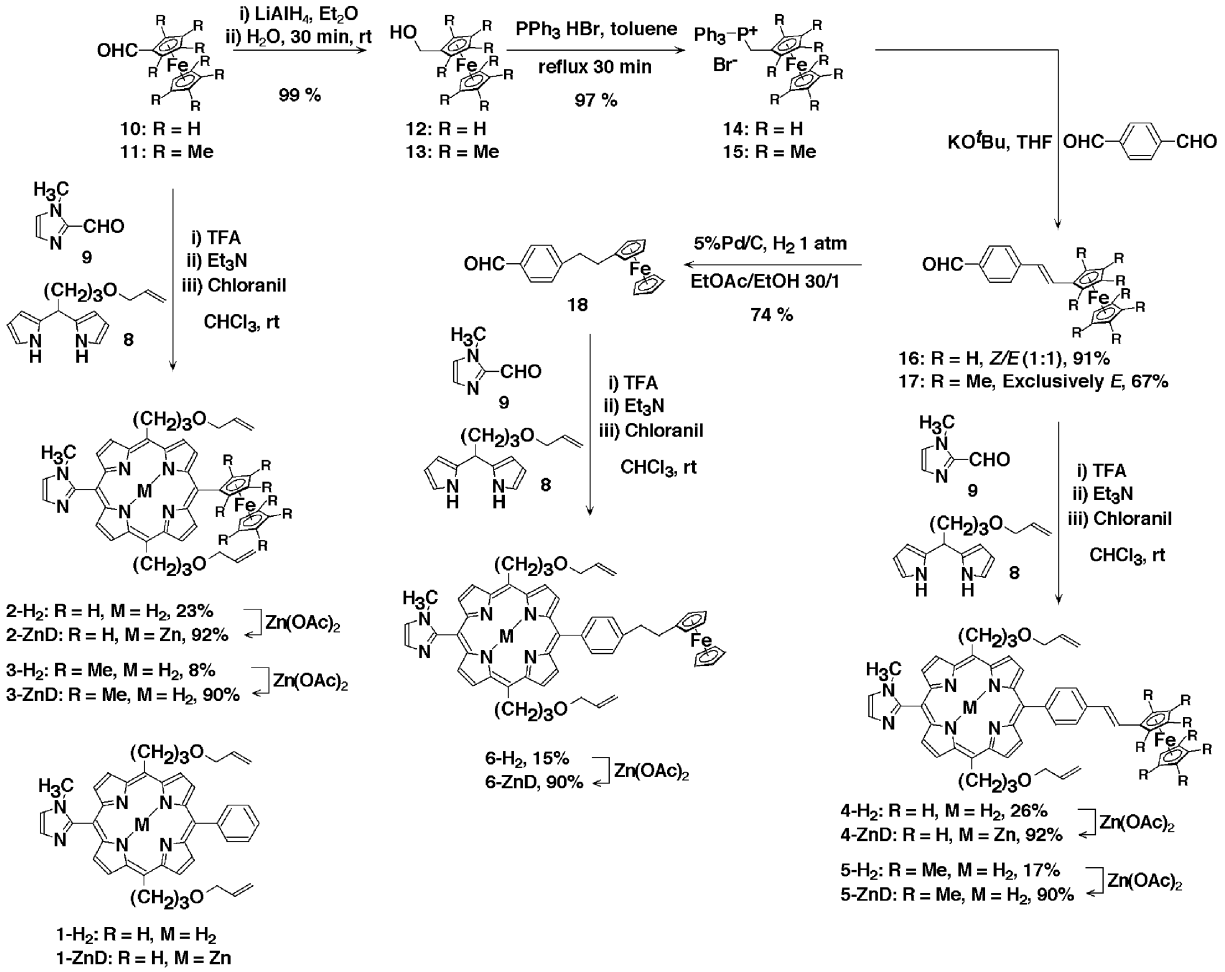


**Scheme 2** Synthetic route to *meso*-substituted ferrocene-functionalized Zn imidazolyl-porphyrins (**2-ZnD** to **6-ZnD**).



dipyrromethane **8**[17] and 1-methyl-2-imidazolecarboxaldehyde **9**.[18] Ferrocenecarboxaldehyde **10**[19] was synthesized according to a literature procedure. Its octamethyl derivative **11**[20]was synthesized in good yield by a modified literature procedure starting from diethyl ketone and acetaldehyde followed by using a $FeCl_2 \cdot 1.5THF$ adduct as a metalating agent (see supplementary data†). To form the target porphyrin a mixed condensation of ferrocene carbaldehyde **10**, 1-methyl-2-imidazolecarboxaldehyde **9** and *meso*-(3-allyloxypropyl)dipyrromethane **8** was carried out in the presence of TFA at room temperature for 5 h. The resultant intermediate was neutralized with triethylamine ($Et_3N$) and subsequently oxidized with *p*-chloranil giving the crude product comprising free base porphyrins. The desired free base porphyrin **2-H$_2$** was obtained in 23% yield after chromatographic separation from 5,15-bis(3-allyloxypropyl)-10,20-bis(ferrocenyl)porphyrin (*bis*Fc-Por) and 5,15-bis(3-allyloxypropyl)-10,20-bis(1-methylimidazol-2-yl)porphyrin (*bis*Im-Por). The free base porphyrin **2-H$_2$** was treated with zinc acetate and after final purification the title porphyrin **2-ZnD** was obtained in 92% yield.

Following a similar procedure, 2,2′,3,3′,4,4′,5,5′-octamethylferrocenecarboxaldehyde **11** afforded the free base porphyrin **3-H$_2$** in 8% yield, and gave the title compound **3-ZnD** in 90% yield on subsequent Zn metalation. The heavy substitution of octamethylferrocene makes it less reactive in comparison to ferrocene itself and this resulted in a significant recovery of the unreacted starting material (37%). When the amount of starting material recovered is taken into account, the yield increases to 12%. Steric hindrance prevented the formation of 5,15-bis(3-allyloxypropyl)-10,20-bis(2,2′,3,3′,4,4′,5,5′-octamethylferrocenyl)porphyrin. This is the first time that a sterically hindered octamethylferrocenyl group has been directly connected to a porphyrin ring by a covalent bond. The neutralization of this acidic reaction medium prior to *p*-chloranil oxidation should be carried out with care as the octamethylferrocene group is readily oxidized (0.05 V *vs* Ag/AgCl) when compared to ferrocene itself (oxidation potential 0.48 V *vs* Ag/AgCl in dichloromethane). TLC and MALDI-TOF MS analysis of the crude reaction mixtures showed no signs of the scrambling of the *meso*-substituents in any of these reactions. The porphyrins synthesized, **2-ZnD** and **3-ZnD**, were fully characterized by spectral analysis, including $^1$H NMR, $^{13}$C NMR, UV, IR and MALDI-TOF MS. The analyses of all the compounds were found to be in satisfactory agreement with their suggested structures.

$^1$H NMR of the free base porphyrin is normal in all respects. In compound **2-H$_2$**, a sharp singlet at 10.3 ppm was assigned to the β-CH proton of the porphyrin adjacent to the ferrocene

moiety. The peak shifted to a lower field due to the increased anisotropic effect and van der Waals deshielding caused by the ferrocenyl group in comparison to the reference sample **1-H$_2$**, in which the β-CH protons appeared at 9.54 ppm as a doublet. The inner –NH proton appears in the shielded region at −2.25 ppm, suggesting that **2-H$_2$** retains its aromatic character upon ferrocene substitution at the *meso* position of the porphyrin. The ferrocenyl group resonates in the region 5.50–4.15 ppm. The ferrocenyl ring protons that are directly linked to porphyrin moiety are inequivalent and appeared as two triplets at 5.50 ($J$ = 1.80 Hz) and 4.84 ($J$ = 1.80 Hz) ppm. In the cyclopentadienyl (Cp) ring which is not linked directly to the porphyrin moiety, all the protons are equivalent and resonate as a sharp singlet at 4.15 ppm. MALDI-TOF mass spectra showed an $m/z$ peak at 771.30 (M + H$^+$).

When Zn is introduced into the free base porphyrin **2-H$_2$** in a non-coordinating solvent, a complementary coordinated cofacial dimer, **2-ZnD**, is formed.[5] Clear evidence for this can be observed in the UV-visible absorption spectrum shown in Fig. 3, which shows the splitting of the Soret band after Zn introduction. The exceptionally strong interaction between the two stacked porphyrins results in one set of β-CH protons being shifted to higher field due to the strong ring current effect of the facing porphyrin. The affected protons appear as a doublet at 5.43 ($J$ = 4.59 Hz). Due to the shielding effect, the imidazolyl protons are shifted to far higher fields and appear at 5.57 and 2.22 ppm as a pair of doublets. The N–Me group appears as a singlet at 1.70 ppm.

Fig. 1a represents the $^1$H NMR spectrum of the free base porphyrin **3-H$_2$**. The substitution of the 2,2′,3,3′,4,4′,5,5′-octamethylferrocene group at the *meso* position of porphyrin **3-H$_2$** results in a substantial downfield shift of the β-CH proton adjacent to the octamethylferrocenyl group. This proton appears as a doublet at 11.6 ppm. This shift is quite significant when compared to compound **2-H$_2$** and reference sample **1-H$_2$**. The inner –NH proton is also shifted significantly upfield and appears as a broad singlet at −2.39 ppm. All the β-pyrrolic protons are quite distinct, reflecting the strong interaction of the two chromophoric groups. All the methyl protons of the octamethylferrocene appear as eight singlets at higher field from 2.17 ppm to 1.60 ppm. The lone –CH proton of the octamethylferrocenyl group appears as a singlet at 4.19 ppm, this is shifted downfield when compared to its parent compound where it appeared as a singlet at 3.45 ppm. After Zn introduction the protons shifted in the usual manner as described for compound **2-ZnD**.

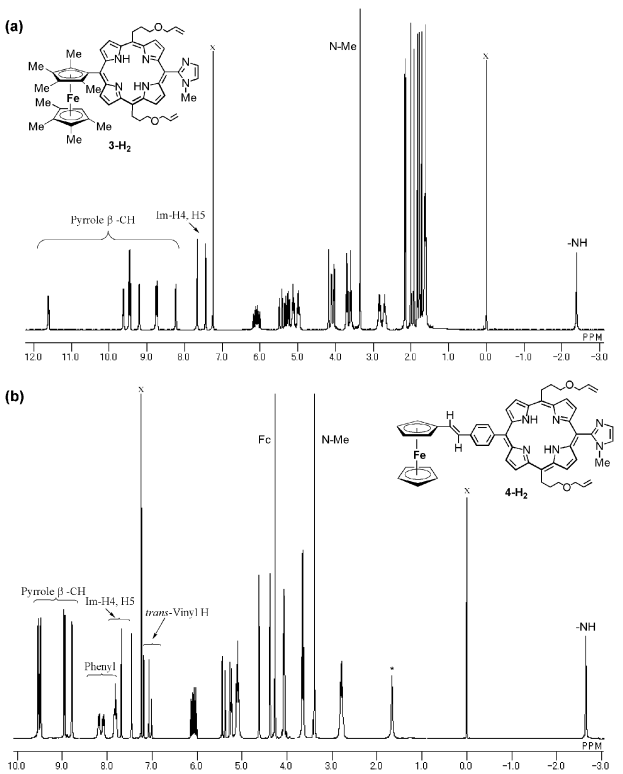


**Fig. 1** $^1$H NMR spectra of free base porphyrins **3-H$_2$** (a) and **4-H$_2$** (b) in $CDCl_3$.

**Ferrocene phenylene-ethenylene-linked porphyrins, 4-ZnD and 5-ZnD.** The established synthetic route for spacer linked olefinic conjugated ferrocenyl porphyrins such as **4-ZnD** and **5-ZnD** employs Wittig and/or Wittig–Horner reactions.[21] The necessary synthons for the stepwise construction of such porphyrins are thus ferrocenecarboxaldehyde, octamethylferrocenecarboxaldehyde and terephthalaldehyde or the hydroxymethyl derivatives as phosphonium progenitors. However, our initial approach towards the Wittig/Wittig–Horner reactions of 2,2′,3,3′,4,4′,5,5′-octamethylferrocenecarboxaldehyde **11** with mono protected {4-(5,5-dimethyl-[1,3]-dioxan-2-yl)-benzyl}triphenylphosphonium bromide **19** and {4-(5,5-dimethy-[1,3]-dioxan-2-yl)benzyl}phosphonic acid diethyl ester **20** did not proceed at all at room temperature due to the steric hindrance and strong electron-donating effect of the methyl group of the octamethylferrocene moiety (Scheme 3). The same reaction with ferrocenecarboxaldehyde **10** gave 80% yield and a 1 : 2 $Z/E$ ratio. This problem was solved by taking the bulky Wittig salts of the corresponding ferrocenyl derivatives (**14**, **15**) and carrying out a subsequent Wittig reaction with terephthalaldehyde. This led to the desired product in exceptionally high yield (see Scheme 3).

Ferrocenecarboxaldehyde **10** and 2,2′,3,3′,4,4′,5,5′-octamethylferrocenecarboxaldehyde **11** were converted to their corresponding alcohols, **12** and **13**, through treatment with $LiAlH_4$ at room temperature in almost quantitative yields. Care should be taken during the addition of the reducing agent, because an excess amount can result in the decomposition of the products. A one-step conversion of these alcohols to Wittig salts **14** and **15** was achieved through treatment with

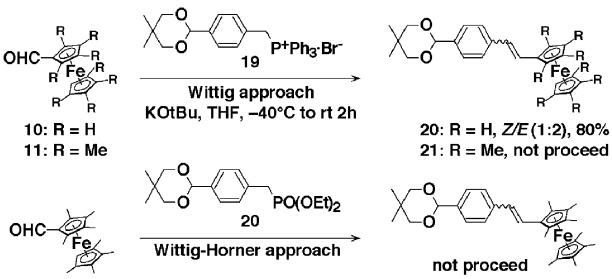


**Scheme 3** Wittig reactions of **11** and **10** with phosphonium progenitors in THF.

 

freshly prepared $PPh_3 \cdot HBr$[22] in toluene with almost quantitative yields. As expected, the Wittig reaction of the ferrocenylmethyl triphenylphosphonium bromide **14** with terephthalaldehyde in the presence of KO-*t*-Bu resulted in a mixture of *cis*/*trans* isomers in 91% yield. The two isomers could be separated by careful chromatography and were obtained in a 1 : 1 *cis* : *trans* ratio. The coupling constants for the olefinic protons in the $^1$H NMR spectra, enabled the unambiguous designation of isomers **16** (*cis* $^3J_{H-H}$ = 12 Hz) and **16** (*trans* $^3J_{H-H}$ = 16.2 Hz). In practice, it is more convenient to treat the *cis* : *trans* mixture with 2 eq. of iodine for 3 h at room temperature, which converts *cis*-**16** to *trans*-**16**, enabling isolation of *trans*-**16** in 99% yield.

The Wittig reaction of (2,2′,3,3′,4,4′,5,5′-octamethylferrocenyl)methyl triphenylphosphonium bromide **15** with excess terephthalaldehyde (6 eq.) in the presence of KO-*t*-Bu afforded exclusively the *E*-"spacered" aldehyde **17** in 67% yield. No *cis* compound or other by-product could be detected by either TLC or $^1$H NMR. This may be due to the high steric demand of the octamethylferrocenyl moiety, which favors the *E*-configuration. The coupling constants for the olefinic protons in the $^1$H NMR spectra allowed for the unambiguous assignment of isomer **17**. The olefinic proton resonance appeared as 16.2 Hz coupled doublets at 7.11 and 6.76 ppm.

Spacer aldehydes **16** and **17** were then employed in porphyrin synthesis through mixed condensation with *meso*-(3-allyloxypropyl)dipyrromethane **8**[17] and 1-methyl-2-imidazolecarboxaldehyde **9**[18] in the presence of TFA. The resultant intermediate was neutralization with $Et_3N$ subsequent *p*-chloranil oxidation resulted in crude products of the free base porphyrins. Column chromatography was used to separate the three porphyrin products, which resulted in the free base porphyrin **4-H$_2$** and **5-H$_2$** in 26% and 17% yields, respectively. The introduction of zinc generated the title porphyrins **4-ZnD** and **5-ZnD** in 92% and 90% yields, respectively. Isomerization of the olefinic double bond or scrambling of *meso* substituents was not observed in these porphyrin syntheses. The exclusive formation of the *trans* olefin was unequivocally determined by $^1$H NMR spectroscopy. For compound **4-H$_2$**, the olefinic proton resonances appear as 16.2 Hz coupled doublets at 7.26 and 7.11 ppm (Fig. 1b). Similarly, the olefinic proton resonances of compound **5-H$_2$** appeared at 7.24 and 7.09 ppm with a coupling constant of 16.2 Hz. Other porphyrin peaks and the allyloxy ether moiety were also quite distinctive.

**Ferrocene phenylene-ethylene-linked porphyrin, 6-ZnD.** Synthesis of **6-ZnD** was completed from the *Z*/*E* mixture of 4-[2-(ferrocenyl)ethenyl]benzaldehyde, **16**. Catalytic hydrogenation of the unsaturated ferrocenyl aldehyde **16** in a solvent mixture of EtOAc-EtOH (30 : 1) produced compound **18** in 74% yield. Reaction of equimolar amounts of 4-[2-(ferrocenyl)ethyl]benzaldehyde **18** and 1-methyl-2-imidazolecarboxaldehyde **9**[18] with *meso*-(3-allyloxypropyl)dipyrromethane **8**[17] in the presence of TFA, followed by neutralization with $Et_3N$ and subsequent chloranil oxidation resulted in crude products containing the free base porphyrins. Purification by $SiO_2$ column chromatography afforded pure **6-H$_2$** in 15% yield. The subsequent zinc insertion yielded the title porphyrin dimer **6-ZnD** in almost quantitative yield.

**Table 1** UV-visible absorption and fluorescence emission spectral data of ferrocene-functionalized Zn-imidazolyl-porphyrins along with reference samples

| Compound | Solvent | Absorption $\lambda_{max}$/nm | Emission $\lambda_{max}$/nm |
|---|---|---|---|
| **1-H$_2$** | $CH_2Cl_2$ | 648, 591, 549, 515, 416 | 720, 653 |
| **1-ZnD** | $CH_2Cl_2$ | 619, 565, 435, 413 | 652, 622 |
| **2-H$_2$** | $CH_2Cl_2$ | 676, 588, 512, 420 | 724, 656 |
| **2-ZnD** | $CH_2Cl_2$ | 649, 578, 442, 422 | —[a] |
| **2-Zn-Py** | Pyridine | 639, 575, 432 | |
| **3-H$_2$** | $CH_2Cl_2$ | 693, 590, 550, 515, 422 | 723, 654 |
| **3-ZnD** | $CH_2Cl_2$ | 649, 567, 440, 418 | —[a] |
| **3-Zn-Py** | Pyridine | 649, 564, 432 | |
| **4-H$_2$** | $CH_2Cl_2$ | 649,597, 552, 517, 420 | 720, 656 |
| **4-ZnD** | $CH_2Cl_2$ | 622, 565, 440, 415 | —[a] |
| **4-Zn-Py** | Pyridine | 615, 562, 431 | |
| **5-H$_2$** | $CH_2Cl_2$ | 646, 600, 548, 514, 418 | 720, 655 |
| **5-ZnD** | $CH_2Cl_2$ | 622, 564, 439, 413 | —[a] |
| **5-Zn-Py** | Pyridine | 615, 565, 431 | |
| **6-H$_2$** | $CH_2Cl_2$ | 650, 591, 552, 517, 418 | 720, 654 |
| **6-ZnD** | $CH_2Cl_2$ | 619, 566, 436, 414 | 680, 623 |
| **6-Zn-Py** | Pyridine | 612, 562, 430 | |

[a] No emission was detected.

### UV-visible absorption spectra and fluorescence emission spectra

UV-visible absorption spectral data for all the synthesized porphyrin-ferrocene dyads are listed in Table 1.

**Ferrocene linked free-base porphyrin dyads, 1-H$_2$–6-H$_2$.** The UV-visible absorption spectra of ferrocenyl- and octamethylferrocenyl- linked porphyrins **2-H$_2$** and **3-H$_2$** exhibit the expected electronic interaction between the porphyrin and ferrocenyl moieties. Fig. 2 shows a comparison between the Q bands of the reference free base compound **1-H$_2$** and the directly connected ferrocenyl porphyrins **2-H$_2$** and **3-H$_2$**. Reference sample **1-H$_2$** displayed well-resolved four Q bands at 648, 591, 549 and 515 nm. Compound **2-H$_2$**, however, showed a shift of one Q band to 676 nm ($\varepsilon$ also increased) and the merging of two Q bands. The merged Q bands appear as broad bands at 588 nm and 512 nm. In addition, the Soret band appears at 420 nm. Compound **3-H$_2$** shows an exceptionally large red shift of Q band at 693 nm, of which longer edge exceeded 900 nm (Fig. 2). The progressive red shift and the broadening of the low-laying Q band for **3-H$_2$** was attributed to the effect of methyl substituents to shift cathodic shift of the redox potential of ferrocene moiety compared to the unsubstituted ferrocenyl-porphyrin **2-H$_2$**. The Q band is located in the longer region than the emission wavelength of **1-H$_2$**, suggesting the intramolecular charge-transfer interaction (redox potentials will be described below). Larger difference of oxidation potentials of ferrocene moiety and that of free-base porphyirn may enhance charge-transfer degree.

No significant electronic interaction exists between the two chromophores in the ground state when the porphyrin unit is connected to the ferrocenyl unit by an phenylene-ethenylene spacer (**4-H$_2$**, **5-H$_2$**, and **6-H$_2$**) (see supplementary data†).

Fig. 4 shows the relative steady state fluorescence spectra in dichloromethane at 25 °C. The effect of introducing ferrocenyl groups is apparent from the sharp drop in fluorescence intensity. The fluorescence of porphyrin **2-H$_2$** and **3-H$_2$** was reduced dramatically to 0.15% that of the free base sample

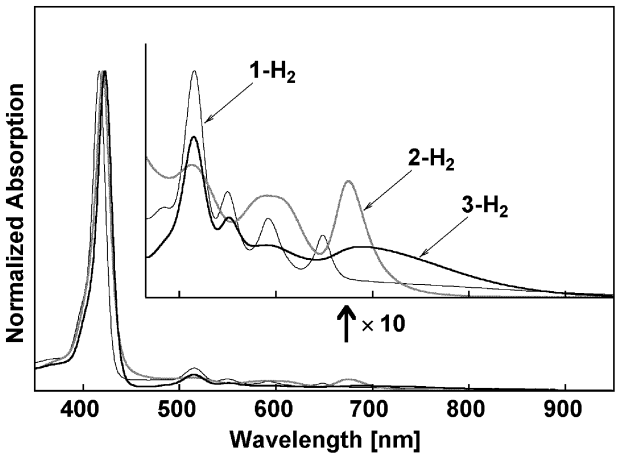


**Fig. 2** Normalized absorption spectra of **1-H$_2$** (solid thin line), **2-H$_2$** (bold dotted line) and **3-H$_2$** (bold solid line) in $CH_2Cl_2$. The inset represents the Q band region magnified by 10 times.

**1-H$_2$** without the ferrocenyl moiety. The phenylene-ethenylene-connected ferrocenyl free base porphyrins **4-H$_2$** and **5-H$_2$** exhibited decreased quenching efficiencies. The decrease of fluorescence intensity in all the ferrocenyl porphyrins is attributed to intramolecular quenching of the porphyrin singlet state by ferrocene. When the conjugation between ferrocene and

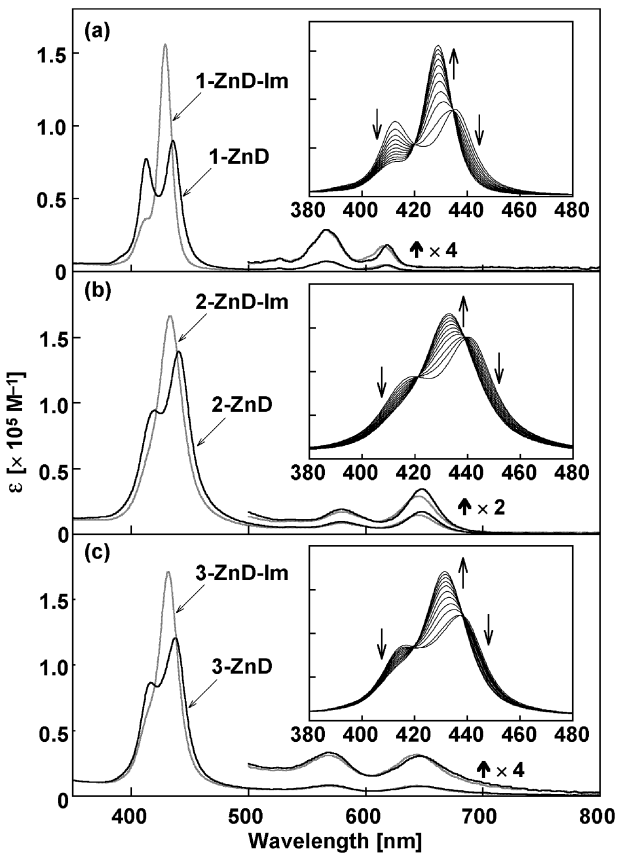


**Fig. 3** Absorption spectra of **1-ZnD**/**1-Zn-Im** (a), **2-ZnD**/**2-Zn-Im** (b), and **3-ZnD**/**3-Zn-Im** (c) in $CH_2Cl_2$. Each spectrum in the Q band region is magnified. The insets show the spectral change in the Soret band region in the course of addition of 1-methylimidazole.

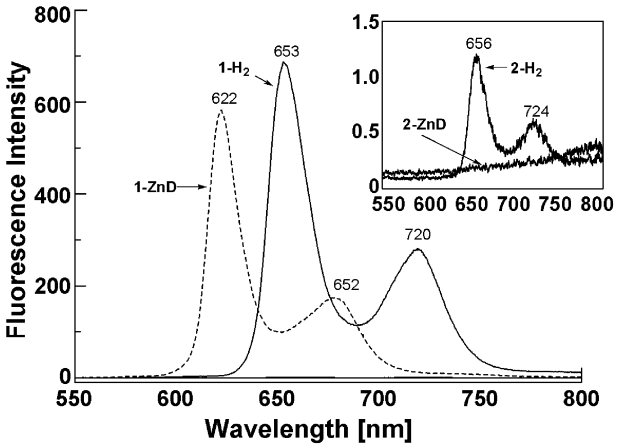


**Fig. 4** Steady state fluorescence spectra of **1-H$_2$** (solid line) and **1-ZnD** (broken line) in $CH_2Cl_2$ at 25 °C. Inset shows emission for **2-H$_2$** and **2-ZnD**. The intensity was normalized to 0.1 absorbance at the excited wavelength of the Soret band, in each case.

porphyrin is disrupted, as in compounds **6-H$_2$**, intramolecular quenching of the porphyrin singlet state by ferrocene dramatically decreased with a corresponding recovery in the fluorescence (Fig. 5). This result indicates that the ferrocenyl group serves as an effective electron donor. The characteristics of the linking group greatly affect the efficiency of fluorescence quenching. Further investigation of fluorescence quenching of the porphyrin moiety by the ferrocenyl group requires fast dynamic measurements, which are currently under investigation.

**Zinc porphyrin dimers, 1-ZnD–6-ZnD.** Ferrocene-functionalized Zn-imidazolyl-porphyrins **2-ZnD**–**6-ZnD** formed a slipped-cofacial dimer in non-coordinating solvents, *e.g.* $CHCl_3$ and $CH_2Cl_2$, by complementary coordination. The Soret band was split by 220 $cm^{-1}$, suggesting an exciton coupling between the two porphyrin chromophores (Fig. 3). The head-to-tail and face-to-face orientations of the transition dipoles $m_{||}$ and $m_{\perp}$ in the slipped-cofacial arrangement

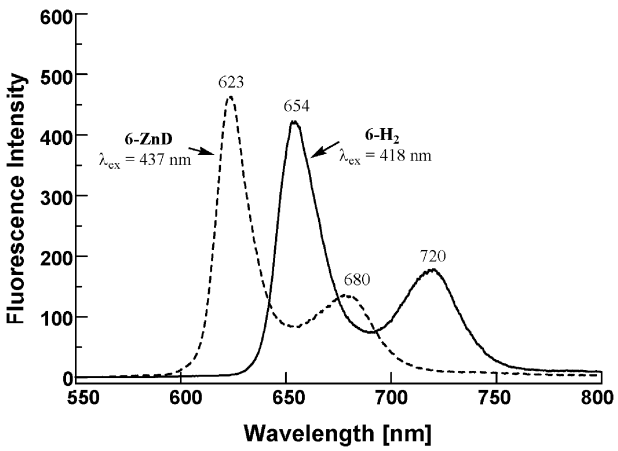


**Fig. 5** Steady state fluorescence spectra of **6-H$_2$** (solid line), **6-ZnD** (broken line) in $CH_2Cl_2$ at 25 °C. The intensity was normalized to 0.1 absorbance at the excited wavelength of the Soret band, in each case.

 

generate bathochromic and hypsochromic shifts of the Soret band, respectively. The association constant of this dimer is extremely high ($>10^{11}$ $M^{-1}$) and the dimer persists even at the detection limit of absorption ($10^{-7}$ M) or fluorescence ($10^{-9}$ M) spectroscopy.[5] The dimer structure can be dissociated to a monomeric unit by adding a competing ligand. On addition of pyridine or 1-methylimidazole as a competing ligand, the split Soret bands are converged into the almost degenerated Soret band at 432 nm through isosbestic points, while the Q bands do not show any significant change. The spectral change clarified that the complementary coordination directed zinc imidazolyl-porphyrins to the slipped-cofacial dimer structure.

The ferrocene substitution at the *meso* position of the porphyrin ring leads to a characteristic feature of the electronic structures. Bathochromic shift of the Q bands depends on the redox potential of the ferrocenyl terminal and the degree of $\pi$-conjugation though the connecting group. When the linker unit contains an aliphatic chain as in **6-ZnD**, the electronic communication is disrupted and the reductive quenching of excited singlet of porphyrin dimer becomes marginal (Fig. 5). Interestingly, the fluorescence was completely quenched in **2-ZnD** and **3-ZnD** (100%). Quantitative quenching was observed for **3-ZnD** and **4-ZnD**, too. This is attributed to electron transfer from the directly linked ferrocenyl moiety to the photoexcited singlet state of porphyrin dimer with exceptionally high efficiencies. The efficient fluorescence quenching in the slipped-cofacial dimer may be correlated with the acceleration of the electron transfer by the decreased reorganization energy of environmental solvent molecules.[24]

### Electrochemical measurements

The redox properties of synthesized porphyrin-ferrocene dyads were examined through cyclic voltammetry (CV) and differential pulse voltammetry (DPV) in dichloromethane. The electrochemical investigation employed a conventional three electrode configuration in dichloromethane with 0.1 M tetrabutylammonium hexafluorophosphate ($^{n}Bu_4N \cdot PF_6$) as a supporting electrolyte at 25 °C.

Fig. 6 presents the cyclic voltammograms of the synthesized ferrocene-functionalized Zn-imidazolyl-porphyrin dimers **2-ZnD**–**5-ZnD**, along with the reference dimer **1-ZnD**. Fig. 7 shows the differential-pulse voltammograms for the equimolar mixture of the ferrocene-functionalized Zn-imidazolyl-porphyrin dimers **2-ZnD**–**5-ZnD** and their dissociated monomers, which were obtained by the addition of 1-methylimidazole **2-Zn-Im**–**5-Zn-Im**, along with the reference sample **1-ZnD** and its monomer **1-Zn-Im**.

**Effect of slipped-cofacial dimer formation.** All of the data are summarized in Table 2. The effect of dimerization on the electronic coupling of Zn-imidazolyl-porphyrins was first investigated for the compounds **1-ZnD**–**6-ZnD** and their corresponding monomers **1-Zn-Im**–**6-ZnD-Im**, each of which was obtained by adding an excess amount of 1-methylimidazole to **1-ZnD**–**6-ZnD**, respectively. The reference monomer **1-Zn-Im** exhibited two irreversible one-electron oxidation waves at 0.6 V and 1.1 V, presumably due to instability of the generated monomeric cation and anion radicals. In the case of dimer

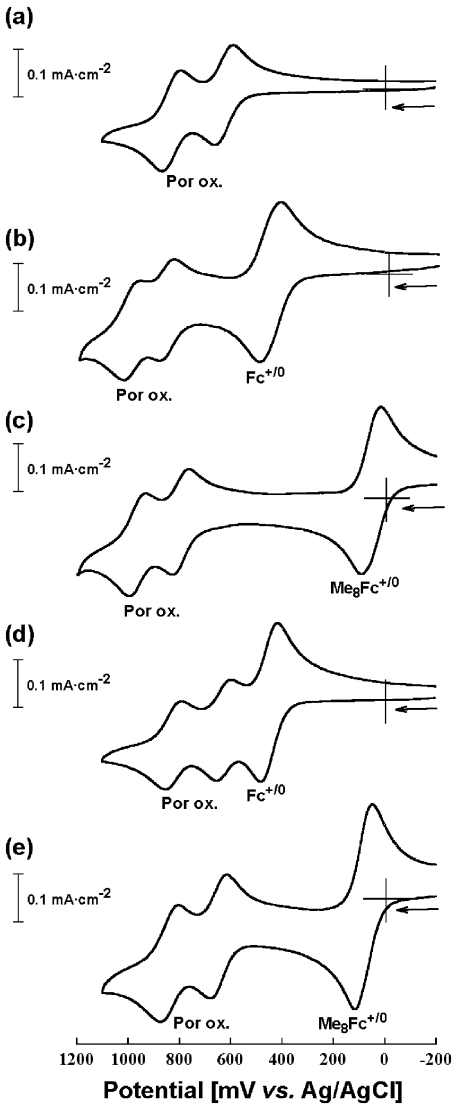


**Fig. 6** Cyclic voltammograms of **1-ZnD** (a), **2-ZnD** (b), **3-ZnD** (c), **4-ZnD** (d), and **5-ZnD** (e) in $CH_2Cl_2$ containing 0.1 M $^{n}Bu_4N \cdot PF_6$ supporting electrolyte at 25 °C with a sweep rate of 100 $mV \cdot sec^{-1}$.

**1-ZnD**, the first oxidation potential of the two porphyrin units in the dimer pair is split into two peaks in the CV ($E_{1/2}$ at 0.63 and 0.83 V), as shown in Fig. 6a.

The significant redox splitting reveals a strong interaction between the redox centers, suggesting that the cation radical generated by the first one-electron oxidation is considerably delocalized over the entire framework of the dimer pair thus raising the potential for the next one-electron oxidation. Further oxidations at more anodic potentials lead to loss of reversibility. Only irreversible processes were observed at 1.2 and 1.5 V. Under controlled anodic potentials, however, dimer **1-ZnD** exhibited a completely reversible stepwise one-electron transfer process (Fig. 6a). It is important to note in comparison of the initial oxidation potentials of **1-ZnD** and **1-Zn-Im** that the dimer formation process does not shift the potential towards easier oxidation. Rather, the second oxidation potential is shifted to a significantly higher value than the first. Similar splittings of the first oxidation wave were observed in

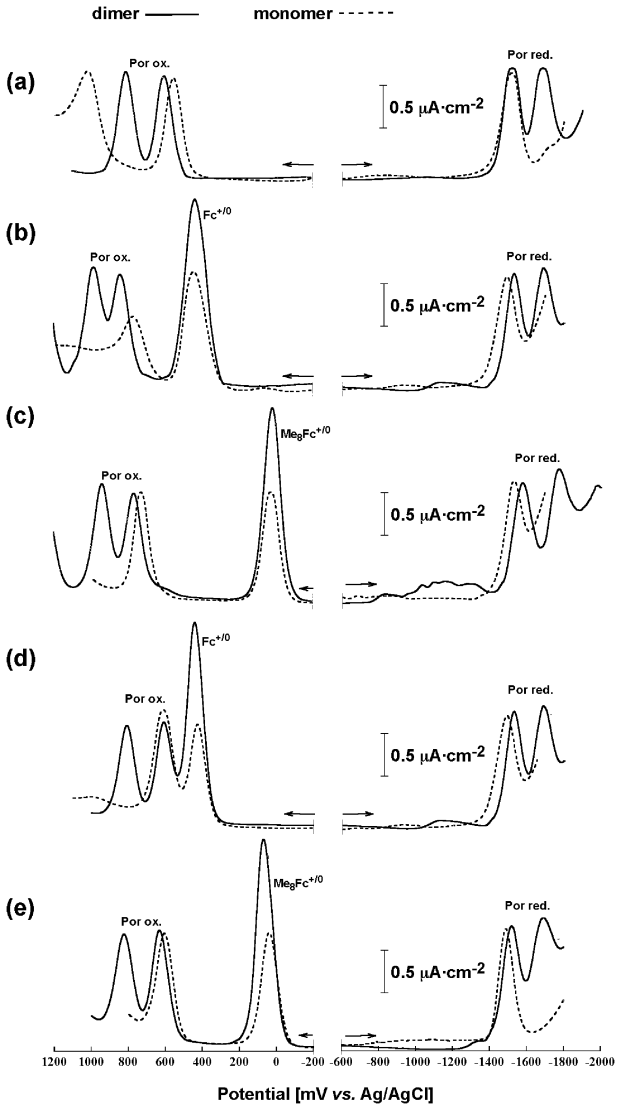


**Fig. 7** Differential-pulse voltammograms of ferrocene-functionalized Zn-imidazolyl-porphyrins along with reference sample without ferrocenyl unit, solid line; coordination dimer and broken line; dissociated monomer. a) **1-ZnD** and **1-Zn-Im**, b) **2-ZnD** and **2-Zn-Im**, c) **3-ZnD** and **3-Zn-Im**, d) **4-ZnD** and **4-Zn-Im**, and e) **5-ZnD** and **5-Zn-Im** in $CH_2Cl_2$ containing 0.1 M $^nBu_4N \cdot PF_6$ supporting electrolyte.

the voltammograms of the ferrocene-functionalized Zn-imidazolyl-porphyrin dimers, **2-ZnD–6-ZnD**, even though the oxidation of ferrocene moiety occurs by a single oxidation step in the dimers.

In the negative potential region, dimer **1-ZnD** exhibited two successive well-defined reversible one-electron reduction waves at 1.55 V and 1.69 V. This also reflects the strong electronic interaction between the two porphyrins in the slipped-cofacial arrangement. Ferrocene-functionalized Zn-imidazolyl-porphyrin dimers, **2-ZnD–6-ZnD**, exhibited split successive one-electron reduction waves from −1.5 V to −1.77 V *vs* Ag/AgCl. The first one-electron reduction of the dimers **2-ZnD–6-ZnD**, occurs at the same or at slightly higher potentials relative to reference sample **1-ZnD** in a similar manner to the oxidation processes. For all of the dimers, reduction of the porphyrin ring was more difficult than for the parent free base porphyrins **2-$H_2$–6-$H_2$** (Table 2). This is consistent with the fact that free base porphyrins generally serve as electron acceptors from zinc porphyrins. Compound **3-ZnD** showed two one-electron reduction waves, at −1.57 V and −1.77 V, representing apparently harder reductions due to the directly connected octamethylferrocene substituents compared to the reference sample **1-ZnD**. This effect is mitigated for the spacer-linked ferrocenyl porphyrins **4-ZnD**, **5-ZnD**, and **6-ZnD**.

In conclusion, the slipped-cofacial dimer formation leads to splittings of the first oxidation and the first reduction waves. This is interpreted in terms of the charge-resonance (intervalance) interaction delocalizing the generated cation radical over the entire π-framework of the special-pair porphyrin dimer.[23] These properties play crucial roles in photoinduced electron transfer to accelerate the charge-separation but to decelerate the charge-recombination.[24] The slipped-cofacial orientation is appropriate as the special-pair model of the natural photosynthesis to provide long-lived charge separation state.

**Effect of ferrocenyl-terminals.** The redox behaviors of **2-ZnD–6-ZnD** were similar and showed characteristic stepwise oxidations for the ferrocenyl moiety followed by the porphyrin rings. Compound **2-ZnD**, where the ferrocenyl group is directly connected to the porphyrin, exhibited well-resolved one-electron oxidations of the two ferrocenes at 0.46 V and split one-electron oxidations of the porphyrin dimer at 0.87 and 1.0 V, respectively, based on the potentials of reference dimer **1-ZnD** and the non-substituted ferrocene. The shift in the porphyrin oxidation potentials is attributed to the fact that the porphyrin oxidations are conducted in the presence of a directly conjugated ferrocenium cation.

The electron-donating abilities of the octamethylferrocenyl group should be noted. The presence of the electron donating methyl groups caused a shift in the oxidation potential of **3-ZnD** by approximately 400 mV to the negative direction compared to **2-ZnD** bearing unsubstituted ferrocene. This result indicates that the octamethylferrocenyl group is more susceptible to oxidation than the ferrocene and is oxidized at a very low oxidation potential, consistent with the well-known effects of methyl substitution. Thus, methyl substitution of the ferrocenyl moiety brings increased solubility, lowered oxidation potential, and amplified donor capacity. The accompanying increased stability of the corresponding ferrocenium cations could be exploited for improving materials used in molecular electronics, solar energy conversion systems and others.

In contrast, when separated by a phenylene-ethenylene spacer from the porphyrin, the ferrocenyl moiety had an almost negligible effect on the porphyrin ring oxidation potentials. In the two compounds **4-ZnD** and **5-ZnD**, the porphyrin oxidation potentials remained almost the same as that of porphyrin without a ferrocenyl group (reference dimer **1-ZnD**). The oxidation potentials of the porphyrins are only marginally affected by the presence of the ferrocenium cation when separated by the phenylene-ethenylene spacer. The redox potentials for **6-ZnD** were nearly identical to those obtained for compound **4-ZnD**, reflecting the minimal perturbation of

 

**Table 2** Half-wave potentials of the reference sample and ferrocenyl-appended porphyrins, free base, Zinc-dimer, and its dissociated monomer with 1-methylimidazole

| Compound | Ferrocene oxidation | Porphyrin oxidation | | Porphyrin reduction | |
|---|---|---|---|---|---|
| | $E_{1/2}{}^{+/0}$/V($\Delta E_p$/mV) | 1st Ox. $E_{1/2}^{0/+}$/V($\Delta E_p$/mV) | 2nd Ox. $E_{1/2}^{2+/+}$/V($\Delta E_p$/mV) | 1st Red. $E_{1/2}^{0/-}$/V($\Delta E_p$/mV) | 2nd Red. $E_{1/2}^{-/2-}$/V($\Delta E_p$/mV) |
| **1-$H_2$** | | 1.0 | 1.2 | −1.20(68) | −1.59(64) |
| **1-ZnD** | | 0.63(76), 0.83(67) | | −1.55(53), −1.70(66) | |
| **1-Zn-Im** | | 0.6 | 1.1 | −1.54(81) | |
| **2-$H_2$** | 0.55(92) | 1.1 | | −1.21(62) | −1.62(90) |
| **2-ZnD** | 0.46(86) | 0.87(56), 1.0(50) | | −1.5, −1.68 | |
| **2-Zn-Im** | 0.44 | 0.77 | | −1.5(106) | |
| **3-$H_2$** | 0.12(87) | 1.1 | | −1.28(61) | −1.64(128) |
| **3-ZnD** | 0.054(70) | 0.80(52), 0.97(60) | | −1.57, −1.77 | |
| **3-Zn-Im** | 0.02(69) | 0.73 | | −1.53 | |
| **4-$H_2$** | 0.45 | 0.91 | 1.20 | −1.2(60) | −1.57(75) |
| **4-ZnD** | 0.45(63) | 0.63(50), 0.83(57) | | −1.50, −1.67 | |
| **4-Zn-Im** | 0.43 | 0.61 | | −1.5 | |
| **5-$H_2$** | 0.076 [a](64) | 0.97(57) | 1.18(99) | −1.23(61) | −1.6(73) |
| **5-ZnD** | 0.084(59) | 0.65(59), 0.84(65) | | −1.52, −1.69 | |
| **5-Zn-Im** | 0.04 | 0.61 | | −1.49 | |
| **6-$H_2$** | 0.39 | 0.9 | 1.21 | −1.21(71) | −1.63(112) |
| **6-ZnD** | 0.45(74) | 0.62(56), 0.82(60) | | −1.55(77), −1.72(85) | |
| **6-Zn-Im** | 0.40 | 0.60 | | −1.54(76) | |
| **$H_2$TPP**[b] | | 1.03 | | −1.23 | −1.55 |
| **Zn-TPP**[b] | | 0.82 | 1.14 | −1.32 | −1.70 |
| **Fc** | 0.48(61) | | | | |
| **$(CH_3)_8$Fc** | 0.057(70) | | | | |

$E_{1/2} = 1/2(E_{pa} + E_{pc})$, $\Delta E_p = E_{pa} - E_{pc}$ (peak potential separation) in CVs $E_p$ = peak potential, $E_{pa}$ = anodic peak potentials, $E_{pc}$ = cathodic peak potential, $E_{1/2}$ = measured half-wave potential by cyclic voltammetry.[a] scan rate 10 mV $s^{-1}$, [b] Ref. 25. In all cases the scan rate is 100 mV $s^{-1}$ unless otherwise stated. Solvent: $CH_2Cl_2$, supporting electrolyte: 0.1 M $^nBu_4N \cdot PF_6$

the porphyrin π-system by the phenylene-ethyl connected ferrocenyl group. Fig. 8 shows the CV and DPV charts for **6-ZnD** along with its monomer **6-Zn-Im**. The charts were superimposed on the same axis for easy comparison.

Judging from the results shown in Table 2, there is no substantial shift of the oxidation potentials of ferrocene or octamethylferrocene moieties by connecting to porphyrin ring except for the directly connected dimers **2-ZnD** and **3-ZnD**, which showed large anodic shifts for the first ring oxidation of the dimer. This potential shift suggests the existence of the strong electronic communication between ferrocenyl moiety and porphyrin plane with close proximity. The difference between the directly connected case (**2-ZnD** and **3-ZnD**) and the separately connected case (**4-ZnD**–**6-ZnD**) is consistent with the spectroscopic properties found in the Q band region.

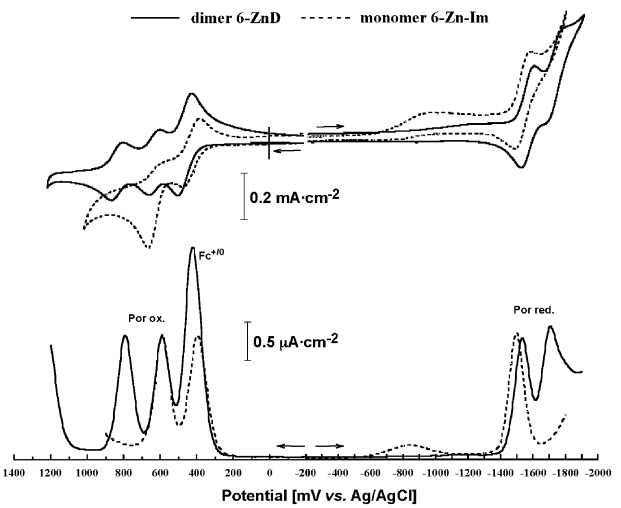


**Fig. 8** CV and DPV of **6-ZnD** and **6-ZnD-Im** in $CH_2Cl_2$ containing 0.1 M $^nBu_4N \cdot PF_6$ as a supporting electrolyte.

The degree of metal–metal interaction (electronic communication) between the two ferrocenyl redox centers in the slipped-cofacial zinc-imidazolyl-porphyrin dimers **2-ZnD**–**6-ZnD** can be judged from the oxidation wave patterns of either CV or DPV. In all cases, only a single oxidation wave was observed, therefore there is no mixed-valence interaction between two ferrocene terminals. However the shift of oxidation potentials of porphyrin rings is enhanced by dimer formation in the directly connected cases, **2-ZnD** and **3-ZnD**, compared with phenylene-ethenylene linked cases, **4-ZnD** and **5-ZnD** (Fig. 7). This indicates that two terminal ferrocenyl groups in the dimer indirectly and weakly communicate through the porphyrin conjugation chain.

**The case of free-base porphyrins.** The half-wave potentials, $E_{1/2}$, of the ferrocenyl-appended free base porphyrins **2-$H_2$**, **3-$H_2$**, **4-$H_2$**, **5-$H_2$** and **6-$H_2$** were recorded in dichloromethane for both oxidation and reduction processes (Table 2). In most cases, a quasi-reversible porphyrin oxidation and two one-electron reversible reductions were observed. In the free base cases, a second reversible reduction wave was observed, which can be compared easily to the corresponding Zn-dimers. Along with the first reduction potential tendencies, described above, these results indicate that the free base porphyrin is more susceptible to porphyrin mono- and dianions compared to the Zn-dimer.

## Conclusions

A one-pot conversion of aldehyde precursors to the corresponding free base porphyrins ($AB_2C$ type), including imidazole and ferrocene as A,C-*meso* substituents, was achieved. Zn insertion produced the title ferrocene-functionalized Zn-imidazolyl-porphyrin dimers **2-ZnD**–**6-ZnD** in reasonably good yields. In this series, ferrocene and octamethylferrocene were substituted at the *meso* position and were connected directly to the porphyrin by phenylene-ethenylene or phenylene-ethyl spacers. The structures were confirmed by spectroscopic analyses and the porphyrins were found capable of serving as a new terminal electron-donor.

UV-visible spectra of **2-ZnD**–**6-ZnD** showed splitting of the Soret band, which suggests the formation of slipped-cofacial dimers and strong excitonic coupling between the two porphyrin units. The porphyrin fluorescence was quenched according to the degree of conjugation: almost completely for direct connections (**2** and **3**), moderately for the phenylene-ethenylenes (**4** and **5**) and marginally for the phenylene-ethyl linkers (**6**). Electrochemical studies of the dimer showed splitting of the first one-electron oxidation/reduction potential of the porphyrin units. In compounds **2-ZnD** and **3-ZnD**, in which the ferrocenyl group is directly connected to the porphyrin, the ferrocenium cation is generated first during oxidation and acts to raise the oxidation potentials of the porphyrin as compared to the reference sample **1-ZnD**. On the other hand, when a phenylene-ethenylene spacer is introduced, the oxidation potentials of the porphyrins are only marginally affected by the presence of the ferrocenium cation.

The interaction between the two ferrocenyl units across the coordination dimer is weak and a single oxidation wave was observed in CV and DPV. The ability to supply a total of four electrons from the dimeric arrays indicates possible applications as controlled electron reservoirs or candidates for a terminal electron donor in a potential cascade. Further studies are currently in progress to exploit these properties for application in molecular devices.

## Experimental

### General

**Apparatus.** $^1H$ and $^{13}C$ NMR spectra were recorded on either a JEOL JNM EX 270, or JEOL ECP-600 (600 MHz) spectrometer. IR spectra (KBr method) were measured with a Nicolet Avatar 320ES FT-IR spectrophotometer. UV-vis spectra were measured by a Shimadzu UV-3100PC spectrophotometer. Fluorescence spectra were recorded on a Hitachi F-4500 spectrometer. MALDI-TOF mass spectra were measured on PerSeptive Biosystems Voyager DE-STR or KRATOS AXIMA with dithranol (Aldrich) as a matrix. Thin-layer chromatography was performed using precoated silica gel glass plates (Silica gel 60 $F_{254}$ E. Merck). Column chromatography was performed using silica gel 60N (spherical, neutral 63–210 μm, KANTO chemical Co., Inc.) and aluminium oxide 90 active basic (0.063–0.200 mm, Merck Ltd.).

**Preparation of reagents.** All chemicals used in the study were of reagent grade. All dry solvents were distilled and stored under $N_2$. Dry THF, $Et_2O$ and toluene were distilled after drying with Na metal and stored under Ar. $CH_2Cl_2$ was distilled from $CaH_2$. Dry DMF was stirred with anhydrous $CuSO_4$ for 2 days and distilled under reduced pressure from $CaH_2$. 1-Methylimidazole was vacuum distilled from KOH. $N_2$, Ar, and $O_2$ gases were of high-quality grades and used without purification. The other chemicals were used without any further purification unless otherwise noted.

**Materials.** *meso*-(3-Allyloxypropyl)dipyrromethane **8**[17], 1-methyl-2-imidazolecarboxaldehyde **9**[18], ferrocenecarboxaldehyde **10**,[19] 2,2′,3,3′,4,4′,5,5′-octamethylferrocenecarboxaldehyde **11**[20] (for details see the Electronic Supplementary Information†), triphenylphosphine hydrobromide[22] were synthesized according to the published procedures.

**Electrochemical measurements.** Electrochemical measurements were carried out in a typical three-electrode configuration connected to a BAS CV-50W potentiostat. The working and the counter electrodes for the cyclic voltammetry (CV) and differential pulse voltammetry (DPV) measurements were a platinum pad (diameter 1.6 mm) and a platinum wire, respectively, and the reference electrode was Ag/AgCl (sat. KCl). This reference electrode was separated from the bulk solution compartment through an agar salt bridge. Tetrabutylammonium hexafluorophosphate ($^nBu_4N \cdot PF_6$, 0.1 M) as a supporting electrolyte recrystallized from ethanol and dried under vacuum at 45 °C prior to use. The sample solutions were deoxygenated by a stream of argon prior to electrochemical measurements.

### Synthesis

**Preparation of zinc porphyrin monomer coordinated by 1-methylimidazole, 1-Zn-Im.** To determine the amount of 1-methylimidazole for monomer formation, reference dimer zinc porphyrin **1-ZnD** (1.0 μmol) and tetrabutylammonium hexafluorophosphate ($^nBu_4N \cdot PF_6$, 0.1 M) were dissolved in dichloromethane (1 mL), and 1-methylimidazole was titrated into this solution (from 1 to 300 eq.), with monitoring by UV-Vis spectroscopy. Following the addition of 1-methylimidazole, the split Soret bands at 413 and 435 nm of the complementary dimer became unified at 425 nm, indicating the dissociation of the dimer into monomer. Under similar condition, a solution of zinc porphyrin monomer **1-Zn-Im**, coordinated by 1-methylimidazole, was prepared for the CV and DPV measurements by dissolving zinc porphyrin dimer **1-ZnD** (1.45 mg, 2.0 μmol), $^nBu_4N \cdot PF_6$ (77.5 mg, 0.2 mmol, 0.1 M) and 1-methylimidazole (300 eq.) in dichloromethane (2 mL).

**Synthesis of 5,15-bis(3-allyloxypropyl)-10-ferrocenyl-20-(1-methylimidazol-2-yl)-porphyrin, 2-$H_2$.** A 200 mL round bottomed flask was charged with ferrocenecarboxaldehyde, 10 (53.5 mg, 0.25 mmol, 0.5 eq.), *meso*-(3-allyloxypropyl)dipyrromethane 8 (122 mg, 0.5 mmol, 1 eq.), 1-methyl-2-imidazolecarboxaldehyde **9** (27.5 mg, 0.25 mmol, 0.5 eq.), and chloroform (50 mL). The mixture was deaerated by bubbling with nitrogen for 10 min and then TFA (0.16 mL, 2.0 mmol, 4 eq.) was added *via* syringe and allowed to stir at room

 

temperature under a nitrogen atmosphere in the dark. The progress of the reaction was monitored by TLC, UV, and MALDI-TOF mass after treatment of the sample with $Et_3N$ and *p*-chloranil. After stirring about 5 h at room temperature, the porphyrin content was found to reach maximum as monitored by UV and then $Et_3N$ (0.21 mL, 2.0 mmol) was added followed by *p*-chloranil (0.184 g, 0.75 mmol, 1.5 eq.) and the reaction mixture was allowed to stir at room temperature for 6 h. The reaction mixture was evaporated to one-third of its initial volume on a rotary evaporator under reduced pressure and then filtered through a silica pad ($CHCl_3$, 1 : 10 acetone : $CHCl_3$). The filtrate was chromatographed over silica gel using hexane : chloroform (1 : 1), chloroform, chloroform : acetone (10 : 1) as eluents. The second green band contained the title porphyrin. Further purification of the title porphyrin was carried out by passing the porphyrin through a basic alumina column (chloroform as an eluent) and reprecipitation from chloroform/hexane to give the pure title compound **2-$H_2$** (44 mg, 23%). TLC [Silica gel, acetone : $CHCl_3$ (1 : 10)]: $R_f = 0.33$. $^1$H NMR (270 MHz, $CDCl_3$): $\delta$ 10.03 (s, 2H; pyrrole-Hβ), 9.44 (d, $J = 5.13$ Hz, 4H; pyrrole-Hβ), 8.73 (d, $J = 4.59$ Hz, 2H; pyrrole-Hβ), 7.67 (d, $J = 1.08$ Hz, 1H; Im-$H_4$), 7.44 (d, $J = 1.08$ Hz, 1H; Im-$H_5$), 6.14–6.02 (m, 2H; allyl-C*H*═), 5.50 (t, $J = 1.80$ Hz, 2H; Cp of Fc), 5.46 (dd, $J = 17.3$, 1.89 Hz, 2H; allyl-$H_{trans}$), 5.29 (dd, $J = 10.4$, 1.7 Hz, 2H; allyl-$H_{cis}$), 5.10 (t, $J = 7.02$ Hz, 4H; -$CH_2$), 4.84 (t, $J =$ 1.80 Hz, 2H; Cp of Fc), 4.15 (s, 5H; Fc-H), 4.11–4.06 (m, 4H; -$CH_2$), 3.67 (t, $J = 6.0$ Hz, 4H; -$CH_2$), 3.37 (s, 3H; N-Me), 2.82–2.74 (m, 4H; -$CH_2$), –2.26 ppm (s, 2H; inner-NH); $^{13}$C NMR (67 MHz, $CDCl_3$): $\delta$ 148.5 (Im-$C_2$), 135.0 (CH-allyl), 132.1–126.8 (br, pyrrole-β), 128.2 (Im-$C_4$), 121.3 (Im-$C_5$), 119.2, 118.8 (*meso*), 116.8 ($CH_2$-allyl), 103.7 (*meso*), 89.8 (*C*-Cp), 77.6 (*C*-Cp), 72.0 (-O*C*$H_2$), 70.6 (*C*H-Cp), 69.2 (-*C*$H_2$-CH═$CH_2$), 68.9 (*C*H-Cp), 37.7 ($CH_2$), 34.4 (N-*C*$H_3$), 31.5 ppm ($CH_2$). MALDI-TOF MS: found $m/z = 771.30$ ($M + H^+$), calculated for $C_{46}H_{46}FeN_6O_2$ 770.30; IR (KBr): $\nu$ 2924, 2854, 1474, 1104, 795, 733 cm$^{-1}$; UV-vis $\lambda_{max}$ ($CH_2Cl_2$) 420, 512, 588, 676 nm; fluorescence, $\lambda_{EM}$ ($CH_2Cl_2$) 656, 724 nm ($\lambda_{Ex}$ 422 nm).

**Synthesis of 5,15-bis(3-allyloxypropyl)-10-(2,2′,3,3′,4,4′,5,5′-octamethylferrocenyl)-20-(1-methylimidazol-2-yl)-porphyrin, 3-$H_2$.** 2,2′,3,3′,4,4′,5,5′-Octamethylferrocenecarboxaldehyde **11** (180 mg, 0.55 mmol, 1.1 eq.), *meso*-(3- allyloxypropyl)dipyrromethane **8** (244 mg, 1.0 mmol, 2.0 eq.), and 1-methyl-2-imidazolecarboxaldehyde **9** (55 mg, 0.5 mmol, 1.0 eq.) were dissolved in chloroform (150 mL) containing 4 Å powdered molecular sieves (2.0 g). The mixture was degassed by bubbling with nitrogen for 10 min and then TFA (0.155 mL, 2.0 mmol, 4.0 eq.) was added and the reaction mixture was allowed to stir at room temperature under a nitrogen atmosphere in the dark. The progress of the reaction was monitored by UV, and MALDI-TOF mass after treatment of the sample with $Et_3N$ and *p*-chloranil. After stirring about 4.5 h at room temperature, the porphyrin content was found to reach maximum as monitored by UV, although MALDI-TOF mass and the TLC analysis showed the presence of large amount of 2,2′,3,3′,4,4′,5,5′-octamethylferrocenecarboxaldehyde **11**. The reaction mixture was then neutralized by adding $Et_3N$ (0.286 mL, 2.1 mmol) followed by a solution of *p*-chloranil (368 mg, 1.5 mmol 1.5 eq.) dissolved in THF (10 mL) and the reaction mixture was allowed to stir at room temperature for 6 h. One third of the chloroform was removed by rotary evaporator under reduced pressure and the residue was filtered through a short silica gel pad (chloroform, then 1 : 10 acetone : chloroform). The second purple band contained the title porphyrin. Much of the starting octamethylferrocenecarboxaldehyde **11** (70 mg, 39%) was recovered as the first eluting orange-red band. Formation of 5,15-bis(3-allyloxypropyl)-10,20-bis(2,2′,3,3′,4,4′,5,5′-octamethylferrocenyl)porphyrin could not be detected by either MALDI-TOF mass or TLC. The title porphyrin **3-$H_2$** was further purified by column chromatography on silica gel using 1 : 4 EtOAc : hexane, chloroform, chloroform : acetone 10 : 1 to give almost 97% pure material. A subsequent flash column chromatography on silica gel 60N (spherical, neutral, 40–50 μm) using 1 : 1 hexane : ethyl acetate led to analytically pure material [35 mg, 8% (12% based on the starting material consumed) as a purple solid. TLC [Silica gel, acetone : $CHCl_3$ (1 : 10)]: $R_f =$ 0.30; $^1$H NMR (270 MHz, $CDCl_3$): $\delta$ 11.60 (d, $J = 4.86$ Hz, 1H; pyrrole-$H_\beta$), 9.62 (d, $J = 4.6$ Hz, 1H; pyrrole-$H_\beta$), 9.43 (t, $J = 5.67$ Hz, 2H; pyrrole-$H_\beta$), 9.19 (d, $J = 4.86$ Hz, 1H; pyrrole-$H_\beta$), 8.74 (dd, $J = 8.91$, 4.86 Hz, 2H; pyrrole-$H_\beta$), 8.22 (d, $J = 4.86$ Hz, 1H; pyrrole-$H_\beta$), 7.67 (d, $J = 1.35$ Hz, 1H; Im-$H_4$), 7.45 (d, $J = 1.35$ Hz, 1H; Im-$H_5$), 6.17–6.00 (m, 2H; allyl-C*H*═), 5.35–5.49 (m, 2H; allyl-$H_{trans}$), 5.22–5.31 (m, 2H; allyl-$H_{cis}$), 5.12, 4.99 (each t, $J = 7.03$ Hz, 4H; -$CH_2$), 4.19 (s, 1H; CH-Cp), 4.10–4.12, 4.03–4.05 (each m, 4H; -O$CH_2$), 3.70, 3.60 (each t, $J = 5.94$ Hz, 4H; -$CH_2$), 3.35 (s, 3H; N-Me), 2.81–2.86, 2.67–2.72 (each m, 4H; $CH_2$), 2.16, 2.14, 2.00, 1.92, 1.83, 1.78, 1.72, 1.60 (8s, 24H; (C$H_3$)$_8$Fc), –2.39 ppm (s, 2H; inner-NH); $^{13}$C NMR (67 MHz, $CDCl_3$): $\delta$ 148.8 (Im-$C_2$), 135.0 (*C*H-allyl), 132.8, 130.9, 129.5, 129.0, 127.9 (br, pyrrole-β), 128.2 (Im-$C_4$), 121.2 (Im-$C_5$), 119.1, 118.6, 117.9 (*meso*), 116.7 (*C*$H_2$-allyl), 103.7 (*meso*), 91.3 (*C*-Cp), 85.3 (*C*-Cp), 84.4 (*C*-Cp), 80.8 (*C*-Cp), 80.7 (*C*-Cp), 80.6 (*C*-Cp), 80.3 (*C*-Cp), 80.2 (*C*-Cp), 80.1 (*C*-Cp), 72.1 (-O*C*$H_2$), 71.9 (CH, Cp), 69.3 ($CH_2$, -*C*$H_2$-CH═$CH_2$), 69.2 (*C*-Cp), 37.8 ($CH_2$), 34.5 (N-*C*$H_3$), 31.4 ($CH_2$), 12.1, 11.9, 11.4, 11.3, 10.3, 10.3, 9.5, 9.4 ppm; MALDI-TOF MS: found $m/z = 882.42$ ($M + H^+$), calculated for $C_{54}H_{62}FeN_6O_2$ 882.43; IR (KBr) $\nu$ 2900, 2850, 1474, 1102, 918, 738 cm$^{-1}$; UV-Vis $\lambda_{max}$ ($CH_2Cl_2$) 422, 515, 550, 590, 693 nm; fluorescence, $\lambda_{EM\ 2}Cl_2$) 654, 723 nm ($\lambda_{Ex}$ 422 nm).

**Synthesis of 5,15-bis(3-allyloxypropyl)-10-ferrocenyl-20-(1-methylimidazol-2-yl)-porphyrinatozinc(II), 2-ZnD.** A solution of zinc acetate dihydrate (25.5 mg, 0.12 mmol) in methanol (1 mL) was added to a solution of 5,15-bis(3-allyloxypropyl)-10-ferrocenyl-20(1-methylimidazol-2-yl)porphyrin **2-$H_2$** (9 mg, 0.012 mmol) in chloroform (3 mL) and the resulting solution was allowed to stir at room temperature for 1 h. After metalation was complete (TLC and MALDI-TOF MS), the reaction mixture was diluted with chloroform (20 mL), washed with aq. $NaHCO_3$ (10 mL) and water (20 mL) and then dried ($Na_2SO_4$), filtered and concentrated in vacuum under reduced pressure. The crude material was next purified by column chromatography on silica gel using chloroform as an eluent to furnish the title porphyrin **2-ZnD** (8.7 mg, 90%) as a purple

solid. $^1$H NMR (270 MHz, $CDCl_3$): $\delta$ 10.27 (d, $J = 4.59$ Hz, 2H; pyrrole-H$\beta$), 9.59 (d, $J = 4.59$ Hz, 2H; pyrrole-H$_\beta$), 8.86 (d, $J = 4.86$ Hz, 2H; pyrrole-H$_\beta$), 6.25–6.13 (m, 2H; $CH_2$=C*H*-), 5.76 (t, $J = 1.62$ Hz, 2H; Cp of Fc), 5.57 (d, $J = 1.62$ Hz, 1H; Im-H$_5$), 5.54 (dd, $J = 10.26$, 1.62 Hz, 2H; allyl-H$_{trans}$), 5.43 (d, $J = 4.59$ Hz, 2H; pyrrole-H$_\beta$), 5.37 (dd, $J = 10.26$, 1.35 Hz, 2H; allyl-H$_{cis}$), 5.17 (t, $J = 7.03$ Hz, 4H; -$CH_2$), 4.93 (t, $J = 1.62$ Hz, 2H; Cp of Fc), 4.32 (s, 5H; Fc-*H*), 4.29–4.22 (m, 4H; -$OCH_2$), 3.94-3.88 (m, 4H; -$CH_2$), 3.10–2.97 (m, 4H; $CH_2$), 2.22 (d, $J = 1.62$ Hz, 1H; Im-H$_4$), 1.70 ppm (s, 3H; N-Me); $^{13}$C NMR (67 MHz, $CDCl_3$): $\delta$ 150.0, 149.5, 148.0 (pyrrole-$\alpha$), 146.2 (Im-$C_2$), 135.3 (*C*H-allyl), 132.3, 128.8, 127.1, 127.0 (pyrrole-$\beta$), 121.6(Im-$C_4$), 119.1, 118.2 (*meso*), 117.4 (Im-$C_5$), 116.7 ($CH_2$-allyl), 96.1 (*meso*), 91.8 (*C*-Cp), 77.9 (*C*H-Cp), 72.1 (-$OCH_2$), 70.6 (*C*H-Cp), 70.10 (-$CH_2$-CH=$CH_2$), 68.5 (*C*H-Cp), 38.5 ($CH_2$), 32.7 ($CH_3$, N-$CH_3$), 31.2 ppm ($CH_2$); MALDI-TOF MS $m/z$ 833.20 ($M + H^+$), 1664.7; calculated for $C_{46}H_{44}FeN_6O_2Zn$ 832.22; IR (KBr): $\nu$ 2922, 2853, 1144, 1104, 987, 788 cm$^{-1}$; UV-Vis $\lambda_{max}$ ($CH_2Cl_2$) 422, 442, 578, 649 nm.

**Synthesis of 5,15-bis(3-allyloxypropyl)-10-(2,2′,3,3′,4,4′,5,5′-octamethylferrocenyl)-20-(1-methylimidazol-2-yl)-porphyrinato-zinc(II), 3-ZnD.** Following the similar procedure described for compound **2-ZnD**, free base sample **3-H$_2$** (9 mg, 0.012 mmol) was reacted with $Zn(OAc)_2 \cdot 2H_2O$ (25.5 mg, 0.12 mmol) in chloroform : methanol (3 : 1) for 3 h to afford the title metalated porphyrin **3-ZnD** (8.7 mg, 90%) as a purple solid after purification. $^1$H NMR (270 MHz, $CDCl_3$): $\delta$ 11.39 (s, 1H; pyrrole-H$_\beta$), 9.69 (s, 1H; pyrrole-H$_\beta$), 9.40 (s, 1H; pyrrole-H$_\beta$), 8.86 (m, 2H; pyrrole-H$_\beta$), 8.61 (s, 1H; pyrrole-H$_\beta$), 6.27–6.12 (m, 2H; allyl-C*H*=), 5.47–5.58 (m, 2H; allyl-H$_{trans}$), 5.42 (d, $J = 1.35$ Hz, 1H; Im-H$_5$), 5.40 (d, $J = 4.6$ Hz, 1H; pyrrole-H$_\beta$), 5.30–5.38 (m, 2H; allyl-H$_{cis}$), 5.24, 5.15 (each m, 4H; -$CH_2$), 4.62 (s, 1H; C*H*-Cp), 4.26–4.19 (m, 4H; -$OCH_2$), 3.95-3.87 (m, 4H; -$CH_2$), 3.01–3.04 (m, 4H; $CH_2$), 2.16, 2.11, 2.01, 1.91, 1.78, 1.73.1.65, 1.60 (8s, 24H; ($CH_3$)$_8$Fc), 2.14 (d, $J = 1.08$ Hz, 1H; Im-H$_4$); 1.67 ppm (s, 3H; N-Me); $^{13}$C NMR (67 MHz, $CDCl_3$): $\delta$ 151.1, 149.8, 148.9, 147.4 (pyrrole-$\alpha$), 146.1 (Im-$C_2$), 135.2 (C*H*-allyl), 133.8, 131.9, 128.6, 127.4 (pyrrole-$\beta$), 121.5 (Im-$C_4$), 118.9, 118.3, 117.1 (*meso*), 117.5, (Im-$C_5$), 116.5 ($CH_2$, allyl), 96.0 (*meso*), 81.0 (*C*-Cp), 80.1 (*C*-Cp), 77.8 (*C*-Cp), 72.0 (-$OCH_2$), 71.9 (*C*-Cp), 70.1 (-$CH_2$-CH=$CH_2$), 70.0 (*C*-Cp), 38.5 ($CH_2$), 34.6 ($CH_3$, N-$CH_3$), 31.6 ($CH_2$) 14.1, 12.8, 11.7, 11.5, 11.3, 10.3, 9.6, 9.5 ppm; MALDI-TOF MS: Found $m/z$ = 944.34 ($M + H^+$), calculated for $C_{54}H_{60}FeN_6O_2Zn$ 944.34, IR(KBr): $\nu$ 2921, 2851, 1459, 1284, 1104, 1074, 986, 787 cm$^{-1}$; UV-Vis $\lambda_{max}$ ($CH_2Cl_2$) 418, 440, 567, 649 nm.

**Synthesis of ferrocenemethanol, 12.** In a round bottomed flask fitted with a water condenser, Ar inlet dropping funnel, and magnetic stirring bar were placed ferrocenecarboxaldehyde **10** (400 mg, 1.87 mmol) and freshly distilled anhydrous diethyl ether (20 mL). A mixture of $LiAlH_4$ (44.0 mg, 1.16 mmol) in anhydrous diethyl ether (5 mL) was then added dropwise *via* the dropping funnel while purging the system with a slow stream of argon. The addition was stopped when the color of the reaction mixture changed from orange-red to yellow (addition of excess $LiAlH_4$ results in decomposition of the product), and the mixture was stirred at room temperature for additional 30 min. A solution of $NH_4Cl$ (500 mg) in $H_2O$ (5 mL) was then slowly added to the above mixture. The ether layer was separated, and the aqueous layer extracted by diethyl ether (2 × 20 mL). The combined organic layer was washed with water (10 mL) and brine (10 mL), and dried over anhydrous $Na_2SO_4$. Evaporation of the solvent on a rotary evaporator gave the title compound **12** in almost quantitative yield (400 mg) as a yellow crystalline solid. TLC [Silica gel, $CHCl_3$]: $R_f = 0.22$; $^1$H NMR (270 MHz, $CDCl_3$): $\delta$ 4.34 (d, 2H; -$CH_2$); 4.32 (s, 2H; Fc-H), 4.24 (s, 2H; Fc-H), 4.18 (s, 5H; Fc-H); $^{13}$C NMR (67 MHz, $CDCl_3$): $\delta$ 88.12, 68.36, 68.22, 67.88, 60.55 ppm; IR (KBr): $\nu$ 3224 (OH), 2953, 1451, 1380, 1236, 1189, 1102, 1040, 991, 924 cm$^{-1}$.

**Synthesis of 2,2′,3,3′,4,4′,5,5′-octamethylferrocenemethanol, 13.** Following the same conditions as described for compound **12**, samples of **11** (0.320 g, 0.98 mmol, in 12 mL diethyl ether), lithium aluminium hydride (23 mg, 0.61 mmol in 4 mL diethyl ether) were reacted to give the desired product **13** in 99.5% (0.320 g) as yellow solid. Mp 180 °C, TLC [Silica gel, EtOAc : hexane (1 : 2)]: $R_f = 0.2$; $^1$H NMR (270 MHz, $CDCl_3$) $\delta$ 4.37 (d, 2H, $J = 4.6$ Hz; -$CH_2$), 3.34 (s, 1H; Cp-H), 1.81 (s, 6H; $CH_3$), 1.73 (s, 6H; $CH_3$), 1.70 (s, 6H; $CH_3$), 1.65 (s, 6H; $CH_3$); $^{13}$C NMR ($CDCl_3$, 67 MHz): $\delta$ 80.73, 80.40, 80.27, 79.54, 70.15, 58.12, 11.35, 9.69, 9.53, 9.48 ppm; IR (KBr): $\nu$ 3238 (OH), 3057, 2963, 2942, 2899, 1448, 1378, 1028, 980, 994, 449 cm$^{-1}$.

**Synthesis of ferrocenylmethyltriphenylphosphonium bromide, 14.** A mixture of ferrocenemethanol **12**, (350 mg, 1.62 mmol), triphenylphosphine hydrobromide, $PPh_3$·HBr (556 mg, 1.62 mmol) and toluene (28 mL) freshly distilled from sodium was refluxed for 30 min until separation from the azeotropic condensate was complete in a Dean–Stark trap. On cooling a yellow solid precipitated, which was filtered off and washed with ether (10 mL) and dried. The organic yellow filtrate, which contains some by-products, was reduced in volume (to about 5 mL) and extracted with water (50 mL). The aqueous layer was washed with ether (10 mL) and re-extracted with chloroform (2 × 50 mL). The chloroform layer was combined, and the solvent was evaporated to give some additional products. Yield: 0.850 g, 97% of yellow air-stable microcrystalline solid. $^1$H NMR (270 MHz, $CDCl_3$): $\delta$ 7.77, 7.74 (m, 15H; Ar-H); 5.10 (brs, 2H; -$CH_2$), 4.36 (s, 5H; Fc-H), 4.04 (s, 2H; Fc-H), 3.97 ppm (s, 2H; Fc-H); $^{13}$C NMR ($CDCl_3$, 67 MHz): $\delta$ 134.72, 134.68, 133.96, 130.02, 129.83, 118.28, 117.04, 70.44, 69.81, 68.70 ppm; IR (KBr): $\nu$ 3045, 2984, 2845 (Ar), 1435, 1110, 996, 842, 739, 690 cm$^{-1}$; UV-vis $\lambda_{max}$ ($CHCl_3$) 332, 460 nm.

**Synthesis of (2,2′,3,3′,4,4′,5,5′-octamethylferrocenyl)-methyl]triphenylphosphonium bromide, 15.** In a similar reaction procedure as that described for compound **14**, a mixture of 2,2′,3,3′,4,4′,5,5′-octamethylferrocenemethanol **13** (1.3 g, 3.96 mmol), triphenylphosphine hydrobromide (1.360 g, 3.96 mmol) in toluene (120 mL) freshly distilled from sodium resulted in the desired Wittig salt **14** (2.5 g, 97%) as yellow crystalline material. Mp 213 °C; $^1$H NMR ($CDCl_3$, 270 MHz): $\delta$ 7.62, 7.70, 7.83, 7.86 (m, 15H; Ar-H), 4.1 (brs, 2H; $CH_2$),

 

3.92 (brs, 1H; Cp-H), 1.81, 1.41, 0.83 ppm (brs, 24H); $^{13}$C NMR (67 MHz, $CDCl_3$): $\delta$ 135.03, 134.30, 129.92 ($C_6H_5$), 10.95, 9.65, 8.98 ppm ($CH_3$ and $CH_2$); MALDI-TOF MS: $m/z$ 573.5 ($M + H^+$); IR (KBr): $\nu$ 3053, 2960, 2940, 2899, 2853, 1585, 1481, 1437, 1380, 1106, 1031, 996, 863, 754, 740, 713, 692, 511, 499, 472, 449 cm$^{-1}$; UV-vis $\lambda_{max}$ ($CHCl_3$) 267, 273, 398 nm.

**Synthesis of 4-[2-(ferrocenyl)ethenyl]benzaldehyde, 16.** A Schlenk vessel was charged with a Wittig salt of ferrocenylmethyltriphenylphosphonium bromide **14** (0.500 g, 0.924 mmol) and dry THF (10 mL) under an argon atmosphere. The resulting suspension was cooled to −40 °C and KO-*t*-Bu (0.114 g, 1.16 mmol, 1.1 eq.) was added in one portion, and the red suspension was stirred for 10 min in an ice/water bath. Subsequently, terephthalaldehyde (0.496 g, 3.7 mmol, 4 eq.) was added, and the deep purple solution was allowed to warm at room temperature during 2 h. At this point TLC (Silica, EtOAc : hexane, 1 : 10) showed no further reaction. The solvent was removed on a rotary evaporator under reduced pressure and the residue washed with aqueous saturated ammonium chloride solution (35 mL) and extracted with diethyl ether (4 × 50 mL). The combined organic layer was dried, filtered and concentrated *in vacuo*. TLC indicated formation of the both isomer *cis*/*trans* (*Z*/*E*) in a 1 : 1 ratio. The crude material was next chromatographed on silica gel (1 : 10, EtOAc : hexane) to furnish the both isomers separately (overall, 0.264 g, 91% yield, *Z*/*E*, 1 : 1). *cis* (*Z*)-Isomer, pink gummy liquid, TLC [Silica gel, EtOAc : hexane, (1 : 10)]: $R_f$ = 0.35; *trans* (*E*)-isomer pink-orange crystalline solid, TLC [Silica gel, EtOAc : hexane, (1 : 10)]: $R_f$ = 0.28; $^1$H NMR (270 MHz, $CDCl_3$, *cis*-isomer): $\delta$ 9.97 (s, 1H; CHO), 7.80 (d, $J$ = 8.1 Hz, 2H; Ar-H), 7.51 (d, $J$ = 8.1 Hz, 2H; Ar-H), 6.49 (d, $^3J_{cis(^1H-^1H)}$ = 12.0 Hz, 1H; -C*H*═C), 6.44 (d, $^3J_{cis(^1H-^1H)}$ = 12.0 Hz, 1H; -C═C*H*), 4.21 (t, $J$ = 1.62 Hz, 2H; Fc-H), 4.18 (t, $J$ = 1.62 Hz, 2H; Fc-H), 4.11 ppm (s, 5H; Fc-H); UV-vis $\lambda_{max}$ ($CHCl_3$) 318 nm. $^1$H NMR (270 MHz, $CDCl_3$, *trans*-isomer): $\delta$ 9.97 (s, 1H, CHO), 7.84 (d, $J$ = 8.1 Hz, 2H, Ar-H), 7.57 (d, $J$ = 8.37, 2H; Ar-H), 7.10 (d, $^3J_{trans(^1H-^1H)}$ = 16.2 Hz, 1H; -C*H*═C), 6.75 (d, $^3J_{trans(^1H-^1H)}$ = 16.2 Hz, 1H; -C═C*H*), 4.51 (d, $J$ = 1.89 Hz, 2H; Fc-H), 4.36 (d, $J$ = 1.89 Hz, 2H; Fc-H), 4.16 ppm (s, 5H; Fc-H), $^{13}$C NMR (67 MHz, $CDCl_3$): $\delta$ 191.37, 143.88, 134.47, 131.38, 130.21, 125.93, 124,43, 82.18, 69.74, 69.36, 67.33 ppm; MALDI-TOF MS: $m/z$ = 316; IR (KBr): $\nu$ 1691, 1593, 1564 cm$^{-1}$; UV-vis $\lambda_{max}$ ($CHCl_3$) 483, 342 nm.

Alternatively, the *cis*-product **16** was converted to the *trans*-product **16** in the following manner. The *cis*-compound **16** (0.132 g, 0.42 mmol) was dissolved in $CHCl_3$ (20 mL) and then $I_2$ (0.212 g, 0.84 mmol, 2 eq.) was added and stirred at room temperature for 3 h. A saturated solution of $Na_2SO_3$ (30 mL) was added and stirred vigorously for 30 min. The organic layer was separated, and the aqueous phase extracted with chloroform (2 × 50 mL). The combined organic layer was washed with water (2 × 100 mL), dried over anhydrous $Na_2SO_4$ and solvent removed *in vacuo* to yield the purple solid. TLC and $^1$H NMR indicated the complete conversion of *cis*-isomer to *trans* isomer. Yield = 131 mg, quantitative. $^1$H NMR is identical to that of *trans*-isomer. This material was used without any further purification for the subsequent porphyrin synthesis.

**Synthesis of 4-[2-(2,2′,3,3′,4,4′,5,5′-octamethylferrocenenyl) ethenyl]benzaldehyde, 17.** Following a similar procedure to that described for the synthesis of compound **16**, samples of Wittig salt (2,2′,3,3′,4,4′,5,5′-octamethylferrocenyl)methyl]triphenylphosphonium bromide **15** (1.23 g, 1.89 mmol) and freshly distilled dry THF (20 mL), KO-*t*-Bu (0.255 g, 2.27 mmol, 1.2 eq.) and terephthalaldehyde (1.52 g, 11.34 mmol, 6 eq.) were reacted for 1.5 h. TLC as well as $^1$H NMR of the crude reaction sample showed formation of the *trans* product only. The crude material was next purified by column chromatography on silica gel using $CHCl_3$ : hexane (2 : 1) to furnish the title compound **16** as a purple solid. Yield = 0.540 g (67%); mp: 93–95 °C; TLC [Silica gel, hexane-ethyl acetate (9 : 1)]: $R_f$ = 0.43; $^1$H NMR (270 MHz, $CDCl_3$): $\delta$ 9.96 (s, 1H; CHO), 7.84 (m, 2H; Ar-H), 7.58 (d, $J$ = 8.37 Hz, 2H; Ar-H), 7.11(d, $^3J_{trans(^1H-^1H)}$ = 16.2 Hz, 1H; -C*H*═C), 6.76 (d, $^3J_{trans(^1H-^1H)}$ = 16.2 Hz, 1H; -C═C*H*), 3.33 (s, 1H; CH of Cp), 1.99, 1.83, 1.75, 1.66 ppm (4s, 24H; $CH_3$ of Cp); $^{13}$C NMR (67 MHz, $CDCl_3$): $\delta$ 191.19 (CHO), 144.85, 134.47, 133.99, 131.99, 130.25, 125.29, 124.45, 82.60, 80.97, 80.81, 79.73, 79.71, 71.40, 11.24, 11.21, 9.93, 9.37 ppm; MALDI-TOF MS: found $m/z$ = 428.1 ($M + H^+$), calculated for $C_{27}H_{32}FeO$ 428.18; IR (KBr): $\nu$ 3059, 2966, 2902, 1687, 1590, 1561, 1306, 1218, 1164, 1030, 968, 863, 821, 793, 502, 471 cm$^{-1}$; UV-vis $\lambda_{max}$ ($CHCl_3$) 363, 532 nm.

**Synthesis of 5,15-bis(3-allyloxypropyl)-10-[4-(2-ferrocenyl) ethenyl]phenyl]-20-(1-methylimidazol-2-yl)-porphyrin, 4-$H_2$.** 4-[2-(Ferrocenyl)ethenyl]benzaldehyde **16** (85 mg, 0.27 mmol,), *meso*-(3-allyloxypropyl)dipyrromethane **8** (132 mg, 0.54 mmol) and 1-methyl-2-imidazolecarboxaldehyde **9** (30 mg, 0.27 mmol) were dissolved in chloroform (60 mL). The mixture was degassed by bubbling with nitrogen for 10 min and then TFA (0.083 mL, 1.1 mmol) was added *via* syringe and the reaction mixture was allowed to stir at room temperature under a nitrogen atmosphere in the dark. The progress of the reaction was monitored by UV, and MALDI-TOF mass after treatment of the sample with $Et_3N$ and *p*-chloranil. After stirring for about 5 h, the porphyrin content was found to reach the maximum as monitored by UV and then the reaction mixture was neutralized by the addition of $Et_3N$ (0.11 mL, 1.1 mmol) followed by the addition of *p*-chloranil (198 mg, 0.81 mmol) dissolved in 10 mL of THF. The reaction mixture was allowed to stir at room temperature for 6 h. One third of the chloroform was removed on a rotary evaporator and the residue was subjected to a short column chromatography on silica gel (chloroform, and then 1 : 10 acetone : chloroform). The second green band contained the target porphyrin **4-$H_2$**. Subsequent purification by silica gel column chromatography using 1 : 4 hexane : ethyl acetate, chloroform, chloroform : acetone (10 : 1) led to almost pure material. Finally, the residue was passed through a short basic alumina pad. Yield = 60 mg, 26%; TLC [Silica gel, acetone : $CHCl_3$ (1 : 10)]: $R_f$ = 0.33; $^1$H NMR (270 MHz, $CDCl_3$): $\delta$ 9.52 (d, $J$ = 5.13, 2H; pyrrole-$H_\beta$), 9.47 (d, $J$ = 5.13 Hz, 2H; pyrrole-$H_\beta$), 8.94 (d, $J$ = 4.86 Hz, 2H; pyrrole-$H_\beta$), 8.78 (d, $J$ = 4.86 Hz, 2H; pyrrole-$H_\beta$), 8.17 (d, $J$ = 7.56 Hz, 1H; Ar-H), 8.07 (d, $J$ = 7.56 Hz, 1H; Ar-H), 7.82 (m, 2H; Ar-H), 7.68 (d, $J$ = 1.08 Hz, 1H; Im-$H_4$), 7.46 (d, $J$ = 1.08 Hz, 1H; Im-$H_5$), 7.19 (d, $^3J_{trans(^1H-^1H)}$ = 16.2

Hz, 1H; -CH=C), 7.01 (d, $^3J_{trans(^1H-^1H)}$ = 16.2 Hz, 1H; C=C*H*-), 6.00–6.15 (m, 2H; allyl-C*H*=), 5.44 (dd, $J$ = 17.01, 1.62 Hz, 2H; allyl-$H_{trans}$), 5.27 (m, $J$ = 10.53, 1.35 Hz, 2H; allyl-$H_{cis}$), 5.10 (t, $J$ = 7.02 Hz, 4H; -$CH_2$), 4.62 (t, $J$ = 1.89 Hz, 2H; Fc-H), 4.38 (t, $J$ = 1.62 Hz, 2H; Fc-H), 4.27 (s, 5H; Fc-H), 4.07 (dd, $J$ = 5.67, 1.35 Hz, 4H; $CH_2$), 3.66 (t, $J$ = 5.67 Hz, 4H; -$CH_2$), 3.39 (s, 3H; N-Me), 2.83-2.74 (m, 4H; $CH_2$), −2.65 ppm (s, 2H; inner-NH); $^{13}$C NMR (67 MHz, $CDCl_3$): $\delta$ 148.8 (Im-$C_2$), 140.8 (Ph), 137.2 (Ph), 135.0 (*C*H-allyl), 134.8 (Ph), 132.0, 130.4, 129.0, 127.6 (br, pyrrole-β), 128.2 (Im-$C_4$), 127.8 (Ph), 125.6 (Ph), 123.9 (Ph), 121.2 (Im-$C_5$), 120.6, 119.2 (*meso*), 116.7 (*C*$H_2$-allyl), 104.1 (*meso*), 83.3 (*C*-Cp), 77.5 (*C*-Cp), 72.0 (-$OCH_2$), 69.3 (*C*H-Cp), 69.2 (-*C*$H_2$-CH=$CH_2$), 68.1 (*C*H-Cp), 67.1, 37.8 ($CH_2$), 34.5 ($CH_3$, N-$CH_3$), 31.4 ppm ($CH_2$); MALDI-TOF MS: found $m/z$ = 873.35 ($M$ + $H^+$), calculated for $C_{54}H_{52}FeN_6O_2$ 872.35; IR (KBr): $\nu$ 2922, 2852, 1104, 797 cm$^{-1}$; UV-Vis $\lambda_{max}$ ($CH_2Cl_2$) 420, 517, 552, 649 nm; fluorescence, $\lambda_{EM}$ ($CH_2Cl_2$) 656, 720 nm ($\lambda_{Ex}$ 420 nm).

**Synthesis of 5,15-bis(3-allyloxypropyl)-10-{4-[2-(2,2′,3,3′,4,4′,5,5′-octamethylferrocenenyl)ethenyl]phenyl}-20-(1-methylimidazol-2-yl)porphyrin, 5-$H_2$.** Following the same reaction procedure as for compound **4-$H_2$**, samples of **17** (215 mg, 0.5 mmol), *meso*-(3-allyloxypropyl)dipyrromethane **8** (245 mg, 1.0 mmol) and 1-methyl-2-imidazolecarboxaldehyde **9** (55 mg, 0.5 mmol) in chloroform (180 mL) were reacted in the presence of TFA (0.16 mL, 2.0 mmol) followed by chloranil (370 mg, 1.5 mmol) oxidation to furnish a mixture of porphyrin products. Purification by column chromatography afforded the title compound **4-$H_2$** in 17% yield. TLC [Silica gel, acetone : $CHCl_3$ (1 : 10)]: $R_f$ = 0.32; $^1$H NMR (270 MHz, $CDCl_3$): $\delta$ 9.53 (d, $J$ = 4.86 Hz, 2H; pyrrole-$H_\beta$), 9.48 (d, $J$ = 4.86 Hz, 2H; pyrrole-$H_\beta$), 8.98 (d, $J$ = 4.60 Hz, 2H; pyrrole-$H_\beta$), 8.78 (d, $J$ = 4.86 Hz, 2H; pyrrole-$H_\beta$), 8.18 (d, $J$ = 8.1 Hz, 1H; Ar-H), 8.10 (d, $J$ = 8.1 Hz, 1H; Ar-H), 7.84 (m, 2H; Ar-H), 7.68 (d, $J$ = 1.08 Hz, 1H; Im-$H_4$), 7.47 (d, $J$ = 1.08 Hz, 1H; Im-$H_5$), 7.19 (d, $^3J_{trans(^1H-^1H)}$ = 16.0 Hz, 1H; -C*H*=C), 7.00 (d, $^3J_{trans(^1H-^1H)}$ = 16.2 Hz, 1H; -C*H*=C), 6.15–6.01 (m, 2H; allyl-C*H*=), 5.45 (dd, $J$ = 17.28, 1.62 Hz, 2H; allyl-$H_{trans}$), 5.28 (dd, $J$ = 10.26, 1.35 Hz, 2H; allyl-$H_{cis}$), 5.11 (t, $J$ = 7.02 Hz, 4H; -$CH_2$), 4.08 (dd, $J$ = 5.4, 1.35 Hz, 4H; -$OCH_2$), 3.66 (t, $J$ = 6.0 Hz, 4H; -$CH_2$), 3.43 (brs, 1H; CH-Cp), 3.40 (s, 3H; N-Me), 2.75–2.84 (m, 4H; $CH_2$), 2.14, 1.90, 1.85, 1.80 (s, $CH_3$, 24H; ($CH_3$)$_8$Fc), −2.63 ppm (brs, 2H; inner-NH); $^{13}$C NMR (67 MHz, $CDCl_3$): $\delta$ 148.7 (Im-$C_2$), 140.2 (Ph), 138.2 (Ph), 134.8 (*C*H-allyl), 134.7 (Ph), 132.0, 130.2, 129.0, 127.4 (br; pyrrole-β), 128.1 (Im-$C_4$), 126.1 (Ph), 123.4 (Ph), 121.2 (Im-$C_5$), 120.8, 120.4, 119.2 (*meso*), 116.7 (*C*$H_2$-allyl), 104.0 (*meso*), 82.0 (*C*-Cp), 81.0 (*C*-Cp), 79.5 (*C*-Cp), 77.1 (*C*-Cp), 71.9 (-$OCH_2$), 71.4 (*C*H-Cp), 69.0 (-*C*$H_2$-CH=$CH_2$), 37.7 ($CH_2$), 34.4 (N-$CH_3$), 31.3 ($CH_2$), 11.3, 11.2, 9.9, 9.5 ppm; MALDI-TOF MS: found $m/z$ = 985.48 ($M$ + $H^+$), calculated for $C_{62}H_{68}FeN_6O_2$ 984.49; IR (KBr): $\nu$ 2940, 2898, 2854, 1104, 1002, 964, 796, 740 cm$^{-1}$; UV-Vis $\lambda_{max}$ ($CH_2Cl_2$) 418, 514, 548, 646 nm; fluorescence, $\lambda_{EM}$ ($CH_2Cl_2$) 655, 720 nm ($\lambda_{Ex}$ 418 nm).

**Synthesis of 5,15-bis(3-allyloxypropyl)-10-[4-(2-ferrocenyl)ethenyl]phenyl}-20-(1-methylimidazol-2-yl)-porphyrinatozinc (II), 4-ZnD.** Following a similar procedure as described for compound **2-ZnD**, reactions of free base porphyrin **4-$H_2$** (23 mg, 0.26 mmol) with $Zn(OAc)_2 \cdot 2H_2O$ (58 mg, 0.26 mmol) in a mixture of $CHCl_3$ : MeOH (10 : 2) resulted the title product (22 mg, 92%) as a light green-purple solid. $^1$H NMR (270 MHz, $CDCl_3$): $\delta$ 9.64 (d, $J$ = 4.6 Hz, 2H; pyrrole-$H_\beta$), 9.11 (d, $J$ = 4.6 Hz, 2H; pyrrole-$H_\beta$), 8.84 (d, $J$ = 4.86 Hz, 2H; pyrrole-$H_\beta$), 8.63 (d, $J$ = 7.56 Hz, 1H; Ar-H), 8.12 (d, $J$ = 7.83 Hz, 1H; Ar-H), 7.99 (d, $J$ = 8.1 Hz, 1H; Ar-H), 7.83 (d, $J$ = 8.1 Hz, 1H; Ar-H), 7.26 (d, $^3J_{trans(^1H-^1H)}$ = 16.2 Hz, 1H; -C*H*=C), 7.11 (d, $^3J_{trans(^1H-^1H)}$ = 16.0 Hz, 1H; C=C*H*-), 6.12–6.26 (m, 2H; allyl-C*H*=), 5.52 (dd, $J$ = 16.47, 1.62 Hz, 2H; allyl-$H_{trans}$), 5.49 (d, $J$ = 1.62 Hz, 1H; Im-H5), 5.41 (d, $J$ = 4.59 Hz, 2H; pyrrole-$H_\beta$), 5.32 (dd, $J$ = 10.53, 1.35 Hz, 2H; allyl-$H_{cis}$), 5.24 (t, $J$ = 7.03 Hz, 4H; -$CH_2$), 4.68 (t, $J$ = 1.62 Hz, 2H; Fc-H), 4.41 (t, $J$ = 1.89 Hz, 2H; Fc-H), 4.32 (s, 5H; Fc-H), 4.22–4.24 (m, 4H; -$OCH_2$), 3.93–3.94 (m, 4H; -$CH_2$), 2.99–3.11 (m, 4H; $CH_2$), 2.14 (d, 1H, $J$ = 1.35 Hz; Im-$H_4$), 1.67 ppm (s, 3H; N-Me); $^{13}$C NMR (67 MHz, $CDCl_3$): $\delta$ 151.0, 149.7, 148.9, 148.0 (pyrrole-α), 146.1 (Im-$C_2$), 142.7 (Ph), 136.7 (Ph), 135.2 (CH-allyl), 132.0, 128.2, 127.2, 127.0 (pyrrole-β), 129.2, 126.1, 121.2 (Im-$C_4$), 119.1 (*meso*), 117.7 (Im-$C_5$), 116.7 (*C*$H_2$-allyl), 96.1 (*meso*), 83.7, 72.1 (-$OCH_2$), 70.1, 69.4 (-*C*$H_2$-CH=$CH_2$), 69.2, 67.1, 38.6 ($CH_2$), 32.7 (N-$CH_3$), 32.2, 31.7 ($CH_2$), 22.74, 14.2 ppm; MALDI-TOF MS: found $m/z$ = 934.38 ($M$ + $H^+$), calculated for $C_{54}H_{50}FeN_6O_2Zn$ 934.26; IR (KBr): $\nu$ 2920, 2852, 1483, 1340, 1104, 1002, 986, 789 cm$^{-1}$; UV-Vis $_{max}$ ($CH_2Cl_2$) 415, 440, 565, 622 nm.

**Synthesis of 5,15-bis(3-allyloxypropyl)-10-{4-[2-(2,2′,3,3′,4,4′,5,5′-octamethylferrocenenyl)ethenyl]phenyl}-20-(1-methylimidazol-2-yl)porphyrinatozinc(II), 5-ZnD.** Following a similar procedure to that described for the synthesis of compound **4-ZnD**, free base porphyrin **5-$H_2$** reacted with $Zn(OAc)_2 \cdot 2H_2O$ in a mixture of $CHCl_3$ : MeOH (30 : 5) for 3 h to afford the title compound **5-ZnD** (24 mg, 90%) as a purple solid after purification. $^1$H NMR (270 MHz, $CDCl_3$): $\delta$ 9.64 (d, $J$ = 4.6 Hz, 2H; pyrrole-$H_\beta$), 9.14 (d, $J$ = 4.60 Hz, 2H; pyrrole-$H_\beta$), 8.95 (d, $J$ = 4.86 Hz, 2H; pyrrole-$H_\beta$), 8.62 (d, $J$ = 8.1 Hz, 1H; Ar-H), 8.11 (d, $J$ = 8.1 Hz, 1H; Ar-H), 7.99 (d, $J$ = 7.29 Hz, 1H; Ar-H), 7.85 (d, $J$ = 7.56 Hz, 1H; Ar-H), 7.24 (d, $^3J_{trans(^1H-^1H)}$ = 16.0 Hz, 1H; -C*H*=C), 7.09 (d, $^3J_{trans(^1H-^1H)}$ = 16.2 Hz, 1H; C=C*H*-), 6.26–6.12 (m, 2H; allyl-C*H*=), 5.55 (dd, $J$ = 10.26, 1.62 Hz, 2H; allyl-$H_{trans}$), 5.49 (d, $J$ = 1.62 Hz, 1H; Im-$H_5$), 5.41 (d, $J$ = 4.86 Hz, 2H; pyrrole-$H_\beta$), 5.35 (dd, $J$ = 10.26, 1.35 Hz, 2H; allyl-$H_{cis}$), 5.24 (m, 4H; -$CH_2$), 4.22–4.24 (m, 4H; -$OCH_2$), 3.91–3.94 (m, 4H; -$CH_2$), 3.52 (brs, 1H; CH-Cp), 3.00–3.12 (m, 4H; $CH_2$), 2.17, 1.92, 1.87, 1.82 (s, 24H; ($CH_3$)$_8$-Fc), 2.14 (d, 1H, $J$ = 1.35 Hz, Im-$H_4$), 1.67 ppm (s, 3H; N-Me); $^{13}$C NMR (67 MHz, $CDCl_3$): $\delta$ 150.9 149.7, 148.9, 147.8 (pyrrole-α), 146.0 (Im-$C_2$), 142.1 (Ph), 137.7 (Ph), 135.2 (*C*H-allyl), 132.0, 129.1, 128.1 126.9 (pyrrole-β), 123.0, 122.9, 121.3, 121.2 (Im-$C_4$), 119.0 (*meso*), 117.6 (Im-$C_5$), 116.7 (*C*$H_2$-allyl), 96.0 (*meso*), 83.7, 72.1 (-$OCH_2$), 70.1, 69.4 (-*C*$H_2$-CH = $CH_2$), 69.2, 67.1, 38.6 ($CH_2$), 32.7 (N-$CH_3$), 32.2, 31.7 ($CH_2$), 22.6, 15.2, 14.1, 10.7, 10.5, 9.3, 8.7 ppm; MALDI-TOF MS: found $m/z$ = 1045.48 ($M$ + $H^+$), calculated for $C_{62}H_{66}FeN_6O_2Zn$ 1045.39; IR (KBr: $\nu$ 2941, 2900, 2853, 1628, 1428, 1340, 1104, 1002, 986, 788, 713 cm$^{-1}$; UV-Vis $\lambda_{max}$ ($CH_2Cl_2$) 413, 439, 564, 622 nm.

 

**Synthesis of 4-(2-ferrocenyl-ethyl)benzaldehyde, 18.** A mixture of 4-[2-(ferrocenyl)ethenyl]benzaldehyde (300 mg, 0.95 mmol) and Pd catalyst (300 mg of 5% Pd on carbon) in a solvent mixture of EtOAc (30 mL) and EtOH (1 mL) was stirred for 1 h at room temperature under an atmosphere of hydrogen [hydrogen gas in balloon]; The color of the reaction mixture gradually changed from orange red to colorless. The reaction was stopped at this point and the mixture was filtered, washed with ethanol and solvent removed *in vacuo*. The crude material was purified by short silica gel column chromatography using 1 : 10 EtOAc : hexane as an eluent. Yield: 235 mg, 74%. TLC [Silica gel, EtOAc : hexane, (1 : 10)]: $R_f = 0.35$; $^1$H NMR (270 MHz, $CDCl_3$): $\delta$ 9.98 (s, 1H; CHO), 7.81 (d, $J =$ 8.1 Hz, 2H; Ar-H), 7.34 (d, $J = 8.1$ Hz, 2H; Ar-H), 4.12 (t, $J =$ 1.62 Hz, 2H; Fc-H), 4.06 (t, $J = 1.62$ Hz, 2H; Fc-H), 4.02 (s, 5H; Fc-H); 2.92 (m, 2H; $CH_2$); 2.70 ppm (m, 2H, $CH_2$).

**Synthesis of 5,15-bis(3-allyloxypropyl)-10-[4-(2-ferrocenyl-ethyl)phenyl]-20-(1-methylimidazol-2-yl)-porphyrin, 6-H$_2$.** Following the same reaction procedure for compound **4-H$_2$**, samples of **18** (230 mg, 0.72 mmol) *meso*-(3-allyloxypropyl) dipyrromethane **8** (353 mg, 1.45 mmol) and 1-methylimidazole aldehyde **9** (80 mg, 0.72 mmol) in chloroform (150 mL) were reacted in the presence of TFA (0.23 mL, 2.89 mmol) followed by chloranil (533 mg, 2.17 mmol) oxidation to furnish a mixture of porphyrin products. Purification by column chromatography afforded the title compound **6-H$_2$** in 15% (95 mg). TLC [Silica gel, acetone : $CHCl_3$ (1 : 10)]: $R_f = 0.28$; $^1$H NMR (270 MHz, $CDCl_3$): $\delta$ 9.54 (d, $J = 5.13$ Hz, 2H; pyrrole-$H_\beta$), 9.49 (d, $J = 4.86$ Hz, 2H; pyrrole-$H_\beta$), 8.90 (d, $J = 5.13$ Hz, 2H; pyrrole-$H_\beta$), 8.80 (d, $J = 4.86$ Hz, 2H; pyrrole-$H_\beta$), 8.15 (d, $J = 7.83$ Hz, 1H; Ar-H), 8.05 (d, $J = 7.56$ Hz, 1H; Ar-H), 7.68 (d, $J = 1.08$ Hz, 1H; Im-$H_4$), 7.56 (m, 2H; Ar-H), 7.47 (d, $J = 1.08$ Hz, 1H; Im-$H_5$), 6.00–6.15 (m, 2H; allyl-C*H*═), 5.44 (dd, $J = 17.28$, 1.62 Hz, 2H; allyl-$H_{trans}$), 5.28 (m, $J =$ 10.26, 1.08 Hz, 2H; allyl-$H_{cis}$), 5.13 (t, $J = 7.3$ Hz, 4H; -$CH_2$), 4.26 (t, $J = 1.89$ Hz, 2H; Fc-H), 4.25 (s, 5H; Fc-H), 4.23 (t, $J =$ 1.62 Hz, 2H; Fc-H), 4.08 (dd, $J = 5.4$, 1.35 Hz, 4H; $CH_2$), 3.68 (t, $J = 5.94$ Hz, 4H; -$CH_2$), 3.39 (s, 3H; N-Me), 3.17–3.23 (m, 2H; $CH_2$), 2.95–3.01 (m, 2H; $CH_2$), 2.81–2.76 (m, 4H; $CH_2$), −2.65 ppm (s, 2H; inner-NH); $^{13}$C NMR (67 MHz, $CDCl_3$): $\delta$ 148.8 (Im-$C_2$), 141.5 (Ph), 139.81 (Ph), 134.9 (*C*H-allyl), 134.2 (Ph), 132.1, 130.3, 129.0, 127.5 (pyrrole-β), 128.2 (Im-$C_4$), 126.9 (Ph), 126.5 (Ph), 121.2 (Ph), 120.8 (Im-$C_5$), 190.2, 119.4 (*meso*), 116.7 (*C*$H_2$-allyl), 104.1 (*meso*), 88.5 (*C*-Cp), 76.5 (*C*-Cp), 71.9 (-$OCH_2$), 69.4 (*C*H-Cp), 69.1 (-*C*$H_2$-CH=$CH_2$), 68.6 (*C*H-Cp), 68.3, 67.3, 54.85, 37.8 ($CH_2$), 34.5 (N-$CH_3$), 32.0 ppm ($CH_2$); MALDI-TOF MS: found $m/z =$ 874.70 ($M + H^+$), calculated for $C_{54}H_{52}FeN_6O_2$ 874.37; UV-Vis $\lambda_{max}$ ($CH_2Cl_2$) 418, 519, 550, 649 nm; fluorescence, $\lambda_{EM}$ ($CH_2Cl_2$) 654, 720 nm ($\lambda_{Ex}$ 418 nm).

**Synthesis of 5,15-bis(3-allyloxypropyl)-10-[4-(2-ferrocenyl-ethyl)phenyl]-20-(1-methylimidazol-2-yl)-porphyrinatozinc(II), 6-ZnD.** Following a similar procedure as described for compound **2-ZnD**, reactions of free base porphyrin **6-H$_2$** (50 mg, 57 μmol) with $Zn(OAc)_2 \cdot 2H_2O$ (250 mg, 1.14 mmol) in a mixture of $CHCl_3$ : MeOH (40 : 5) afforded the title product (49 mg, 92%) light green-purple solid. $^1$H NMR (270 MHz, $CDCl_3$): $\delta$ 9.60 (d, $J = 4.86$ Hz, 2H; pyrrole-$H_\beta$), 9.00 (d, $J =$ 4.32 Hz, 2H; pyrrole-$H_\beta$), 8.89 (d, $J = 4.59$ Hz, 2H; pyrrole-$H_\beta$), 8.53 (d, $J = 7.56$ Hz, 1H; Ar-H), 8.02 (d, $J = 7.83$ Hz, 1H;, Ar-H), 7.67 (d, $J = 8.1$ Hz, 1H; Ar-H), 7.52 (d, $J = 8.1$ Hz, 1H; Ar-H), 6.14–6.19 (m, 2H; allyl-C*H*═), 5.48 (dd, $J =$ 16.47, 1.62 Hz, 2H; allyl-$H_{trans}$), 5.41 (d, $J = 1.62$ Hz, 1H; Im-$H_5$), 5.35 (d, $J = 4.59$ Hz, 2H; pyrrole-Hβ), 5.28 (dd, $J = 10.53$, 1.35 Hz, 2H; allyl-$H_{cis}$), 5.16 (t, $J = 7.03$ Hz, 4H; -$CH_2$), 4.26 (t, $J = 1.62$ Hz, 2H; Fc-H), 4.22 (s, 5H; Fc-H), 4.17 (t, $J = 1.89$ Hz, 2H; Fc-H), 4.15–4.20 (m, 4H; -$OCH_2$), 3.83–3.88 (m, 4H; -$CH_2$), 3.18–3.23 (m, 4H; $CH_2$), 2.90–3.10 (m, 4H; $CH_2$), 2.10 (d, $J = 1.35$ Hz, 1H; Im-$H_4$), 1.60 ppm (s, 3H; N-Me); $^{13}$C NMR (67 MHz, $CDCl_3$): $\delta$ 151.0, 149.7, 149.1 147.9 (pyrrole-α), 146.1 (Im-$C_2$), 141.6 (Ph), 140.8 (Ph), 135.3 (*C*H-allyl), 134.6 (Ph), 132.0, 129.2, 126.9, 126.4 (pyrrole-β), 128.1 (Im-$C_4$), 126.2, 121.4, 119.0 (*meso*), 117.7 (Im-$C_5$), 116.7 (*C*$H_2$-allyl), 96.0 (C, *meso*), 88.8, 72.1 (-$OCH_2$), 70.2, 68.7 (-*C*$H_2$-CH=$CH_2$), 68.4, 67.4, 38.7 ($CH_2$), 32.7 (N-$CH_3$), 32.7, 32.2 ppm ($CH_2$); MALDI-TOF MS: found $m/z = 936.57$ ($M +$ $H^+$), UV-Vis $\lambda_{max}$ ($CH_2Cl_2$) 414, 437, 565, 619 nm, fluorescence, $\lambda_{EM}$ ($CH_2Cl_2$) 623, 680 ($\lambda_{Ex}$ 437 nm).

**Preparation of 2-Zn-Im, 3-Zn-Im, 4-Zn-Im and 5-Zn-Im for electrochemical measurements.** Ferrocene fuctionalized zinc-imidazole-porphyrin dimers **2-ZnD**, **3-ZnD**, **4-ZnD**, **5-ZnD** or **6-ZnD** (2.0 μmol), was dissolved with $^n$Bu$_4$N · PF$_6$ (0.2 mmol, 0.1 M) in dichloromethane (2 mL) and 1-methylimidazole (300 eq.) was added. UV-Vis absorption spectra showed the unification of the split Soret band into a single band at 426 nm, indicating dissociation of the dimer into the monomer. These sample solutions were utilized for electrochemical measurements.

## Acknowledgements

This work was supported by Grant-in-Aids for Scientific Research (A) (No. 15205020) and for Scientific Research on Priority Areas (No. 16033244, Reaction Control of Dynamic Complexes) from Ministry of Education, Culture, Sports, Science and Technology, Japan (Monbu Kagakusho).

## References

1 (*a*) J. Deisenhofer and J. R. Norris, *The Photosynthetic Reaction Center*, Vols. I and II, Academic Press, New York, 1993; (*b*) M. E. Michel-Beyerle, *The Reaction Center of Photosynthetic Bacteria*, Springer, Berlin/Heidelberg, 1996; (*c*) H. van Amerongen, L. Valkunas and R. van Grondelle, *Photosynthetic Excitations*, World Scientific, Singapore, 2000.
2 (*a*) A. Zouni, H.-T. Witt, W. J. Kern, P. Fromme, N. Krauss, W. Sanger and P. Orth, *Nature*, 2001, **409**, 739; (*b*) P. Jordan, P. Fromme, H.-T. Witt, O. Kukas, W. Sanger and N. Krauss, *Nature*, 2001, **411**, 909.
3 (*a*) J. Koepke, X. Hu, C. Muenke, K. Schulten and H. Michel, *Structure*, 1996, **4**, 581; (*b*) K. McLuskey, S. M. Prince, R. J. Cogdell and N. W. Isaacs, *Biochemistry*, 2001, **40**, 8783.
4 (*a*) M. R. Wasielewski, *Chem. Rev.*, 1992, **92**, 435; (*b*) D. Gust, T. A. Moore and A. L. Moore, *Acc. Chem. Res.*, 2001, **34**, 40; (*c*) J. Vasudevan, R. T. Stibrany, J. Bumby, S. Knapp, J. A. Potenza, T. J. Emge and H. J. Schugar, *J. Am. Chem. Soc.*, 1996, **118**, 11676.
5 (*a*) Y. Kobuke and H. Miyaji, *J. Am. Chem. Soc.*, 1994, **116**, 4111; (*b*) Y. Kobuke and K. Ogawa, *Bull. Chem. Soc. Jpn.*, 2003, **76**, 689.
6 (*a*) R. Takahashi and Y. Kobuke, *J. Am. Chem. Soc.*, 2003, **125**, 2372; (*b*) Y. Kuramochi, A. Satake and Y. Kobuke, *J. Am. Chem.*

*Soc*., 2004, **126**, 8668; (*c*) C. Ikeda, A. Satake and Y. Kobuke, *Org. Lett*., 2003, **5**, 4935; (*d*) R. Takahashi and Y. Kobuke, *J. Org. Chem*., 2005, **70**, 2745.
7 (*a*) K. Ogawa, A. Ohashi, Y. Kobuke, K. Kamada and K. Ohata, *J. Am. Chem. Soc*., 2003, **125**, 13356; (*b*) K. Ogawa and Y. Kobuke, *Angew. Chem., Int. Ed*., 2000, **39**, 4070.
8 C. E. D. Chidsey, *Science*, 1991, **251**, 919.
9 (*a*) D. J. Campbell, B. R. Herr, J. C. Hulteen, R. P. Van Duyne and C. A. Mirkin, *J. Am. Chem. Soc*., 1996, **118**, 10211; (*b*) S. Creager, C. J. Yu, C. Bamdad, M. Gozin and J. F. Kayyem, *J. Am. Chem. Soc*., 1999, **121**, 1059; (*c*) T. Kondo, S. Horiuchi, I. Yagi and S. Ye. K. Uosaki, *J. Am. Chem. Soc*., 1999, **121**, 391.
10 A. J. Bard and H. Lund, *Encyclopedia of Electrochemistry of the Elements*, Marcel Dekker, New York, 1979, Vol. 13, p. 3.
11 A. Togni and T. Hyashi, *Ferrocenes*, VCH Verlagsgesellschaft mbH, Weinheim, Germany, 1995, references cited therein.
12 (*a*) M. Hobi, O. Ruppert, V. Gramlich and A. Togni, *Organometallics*, 1997, **16**, 1384; (*b*) J. C. Calabrese, L.-T. Cheng, J. C. Green, S. R. Marder and W. Tam, *J. Am. Chem. Soc*., 1991, **113**, 7227; (*c*) S. Barlow, H. E. Bunting, C. Ringham, J. C. Green, G. U. Bubliz, S. G. Boxer, J. W. Perry and S. R. Marder, *J. Am. Chem. Soc*., 1999, **121**, 3715; (*d*) S. Barlow and D. O. Hare, *Organometallics*, 1996, **15**, 3885; (*e*) B. Bildstein, A. Hradsky, H. Kopaca, R. Malleier and K.-H. Ongania, *J. Organomet. Chem*., 1997, **540**, 127.
13 Ferrocene porphyrin direct linkage: (*a*) D. T. Gryko, F. Zhao, A. A. Yasseri, K. M. Roth, D. F. Bocian, W. G. Kuhr and J. S. Lindsey, *J. Org. Chem*., 2000, **65**, 7356; (*b*) C. Bucher, C. H. Devillers, J.-C. Moutet, G. Royal and E. Saint-Aman, *Chem. Commun*., 2003, 888; (*c*) R. G. Wollmann and D. N. Hendrickson, *Inorg. Chem*., 1977, **16**, 3079; (*d*) S. W. Rhee, B. B. Park, Y. Do and J. Kim, *Polyhedron*, 2000, **19**, 1961; (*e*) S. W. Rhee, H. Y. Na, Y. Do and J. Kim, *J. Inorg. Chim. Acta*, 2000, **309**, 49; (*f*) J. Kim, S. W. Rhee, H. Y. Na, K. P. Lee, Y. Do and S. C. Jeoung, *Bull. Korean Chem. Soc*., 2001, **22**, 1316; (*g*) P. D. W. Boyd, A. K. Burell, W. M. Campbell, P. A. Cocks, K. C. Gordon, G. B. Jameson, D. L. Officer and Z. Zhao, *Chem. Commun*., 1999, 637; (*h*) Ferrocene Linkage with spacer: E. S. Schmidt and T. S. Calderwood, *Inorg. Chem*., 1986, **25**, 3718; (*i*) A. K. Burell, W. M. Campbell, D. L. Officer, S. M. Scott, K. C. Gordon and M. R. McDonald, *J. Chem. Soc., Dalton Trans*., 1999, 3349; (*j*) R. Giasson, E. J. Lee, X. Zhao and M. S. Wrighton, *J. Phys. Chem*., 1993, **97**, 2596; (*k*) N. B. Thornton, H. Wojtowicz, T. Netzel and D. W. Dixon, *J. Phys. Chem*., 1998, **102**, 2101; (*l*) A. K. Burrell, W. M. Campbell and D. L. Officer, *Tetrahedron Lett*., 1997, **38**, 1249.
14 A. Nomoto, H. Mitsuoka, H. Ozeki and Y. Kobuke, *Chem. Commun*., 2003, 1074.
15 A. Nomoto and Y. Kobuke, *Chem. Commun*., 2002, 1104.
16 (*a*) M. Morisue, S. Yamatsu, N. Haruta and Y. Kobuke, *Chem.–Eur. J*., 2005, **11**, 5563; (*b*) M. Morisue, D. Kalita, N. Haruta and Y. Kobuke, submitted.
17 A. Ohashi, A. Satake and Y. Kobuke, *Bull. Chem. Soc. Jpn*., 2004, **77**, 365.
18 L. R. Milgrom, P. J. F. Dempsey and D. Yahioglu, *Tetrahedron*, 1996, **52**, 9877.
19 U. T. Mueller-Weaterhoff, Z. Yang and G. J. Ingram, *J. Organomet. Chem*., 1993, **463**, 163.
20 (*a*) C. M. Fendric, L. D. Schertz, V. W. Day and T. J. Marks, *Organometallics*, 1988, **7**, 1828; (*b*) F. H. Koehler and K. H. Doll, *Z. Naturforsch., B: Anorg. Chem. Org. Chem*., 1982, **37**, 144; (*c*) V. G. Schmitt and S. Ozman, *Chem. Ztg*., 1976, **100**, 143.
21 B. E. Maryanoff and A. B. Reitz, *Chem. Rev*., 1989, **89**, 863.
22 J. D. Surmatis and A. Ofner, *J. Org. Chem*., 1963, **28**, 2735.
23 (*a*) D. E. Richardson and H. Taube, *Inorg. Chem*., 1981, **20**, 1278; (*b*) K. Funatsu, T. Imamura, A. Ichimura and Y. Sasaki, *Inorg. Chem*., 1998, **37**, 4986; (*c*) K. Fukushima, K. Funatsu, A. Ichimura, Y. Sasaki, M. Suzuki, T. Fujihara, K. Tsuge and T. Imamura, *Inorg. Chem*., 2003, **42**, 3187.
24 H. Ozeki, A. Nomoto, K. Ogawa, Y. Kobuke, M. Murakami, K. Hosoda, M. Ohtani, S. Nakashima, H. Miyasaka and T. Okada, *Chem.–Eur. J*., 2004, **10**, 6393.
25 K. M. Kadish, E. van Caemelebecke and G. Royal, in *The Porphyrin Hand Book*, ed. K. M. Kadish, K. M. Smith and R. Guilard, Academic Press, San Diego, USA, 2000, Vol. 8, pp. 1.



 